
Miscibility, Phase Separation, and Mechanism of Phase Separation of Epoxy/Block-Copolymer Blends

29

Hernan Garate, Noé J. Morales, Silvia Goyanes, and Norma B. D'Accorso

Abstract

Incorporating block copolymers into epoxy systems has emerged as a versatile and effective methodology not only to enhance their mechanical properties, but also as an intriguing strategy to design advanced materials with tailored properties. Knowledge of microphase separation mechanisms operating during the development of these materials is essential due to the straight relationship between block copolymer characteristics, epoxy system formulation, and curing conditions with the final nanodomain morphology. This chapter is focused on the thermodynamic and kinetic fundamentals describing microphase separation mechanisms by which the nanodomains are obtained. Moreover, key parameters affecting phase separation mechanisms and morphologies are discussed,

H. Garate (✉)

YPF Tecnología S.A., Ensenada, Buenos Aires, Argentina

IFIBA-CONICET, LP&MC, Departamento de Física, FCEyN-UBA, Ciudad Universitaria, Ciudad Autónoma de Buenos Aires, Argentina

CIHIDECAR-CONICET, Departamento de Química Orgánica, FCEyN-UBA, Ciudad Universitaria, Ciudad Autónoma de Buenos Aires, Argentina

e-mail: hgarate001@gmail.com

N.J. Morales

YPF Tecnología S.A., Ensenada, Buenos Aires, Argentina

e-mail: noe.jmorales@gmail.com

S. Goyanes

IFIBA-CONICET, LP&MC, Departamento de Física, FCEyN-UBA, Ciudad Universitaria, Ciudad Autónoma de Buenos Aires, Argentina

e-mail: goyanes@df.uba.ar

N.B. D'Accorso

CIHIDECAR-CONICET, Departamento de Química Orgánica, FCEyN-UBA, Ciudad Universitaria, Ciudad Autónoma de Buenos Aires, Argentina

e-mail: norma@qo.fcen.uba.ar

explaining how different material properties can be tuned by controlling the nanostructure morphology.

Keywords

Block copolymers • Epoxy system • Polymerization-induced microphase separation • Self-assembly • Miscibility

Contents

Introduction	842
Macro- Versus Microphase Separation Behavior	843
Microphase Separation Mechanisms	848
Microphase Separation During Curing	849
Microphase Separation Before Curing	852
“Tandem-Like” Mechanisms	853
Experimental Strategies to Follow Microphase Separation Mechanism	857
Key Parameters Affecting Mechanisms and Morphologies	859
Epoxy/BCP Composition	859
Number of Block Types	860
Block Sequence	861
Influence of BCP Reactivity	863
Influence of the Hardener	864
Influence of Curing Conditions	866
Impact of Morphology in the Epoxy/BCP Blend Properties	872
Mechanical Properties	873
Thermal Properties	873
Surface Properties	876
Conclusions	877
References	877

Introduction

Block copolymers are a unique class of polymers capable of structuring epoxy systems down to molecular scales (few tens of nanometers). This intriguing ability can be used to design advanced nanostructured polymers with potential technological applications as multifunctional coatings (Esposito et al. 2014), transparent materials with high refractive indices for optical applications (Caseri 2000), low dielectric constant films for microelectronic industry (Hedrick et al. 1998), nanostructured templates for composite materials (Esposito et al. 2013) and porous polymers (Guo et al. 2008), and toughening of polymer networks (Karger-Kocsis et al. 2004; Zhu et al. 2004; Declet-Perez et al. 2015), among others.

With the aim to obtain novel materials with tuned properties, it is crucial to first understand the nanostructuring mechanisms operating during thermoset formation and how these are related to the thermodynamics of epoxy/BCP blends and kinetic conditions dictated by viscosity and curing kinetics. It is possible to adjust the nature of the selected epoxy/BCP blend and establish curing conditions that enable obtaining controlled nanodomain morphologies. Moreover, since there is a close

relationship between morphology, size, dispersion state, and interfacial adhesion between the phases and the ultimate properties of the blends, knowledge of phase separation mechanism in these systems is essential to gain access a myriad of well-defined morphologies and therefore controlled final properties, by tuning epoxy/BCP formulation and curing conditions.

This chapter provides an insight into thermodynamic and kinetic fundamentals of nanodomain formation mechanisms in epoxy/BCP blends which are essential to understand how it is possible to control nanodomain size, shape, and morphology by selecting proper blend formulation and curing conditions. It also provides a discussion of key factors that control the obtained morphologies and describes how a given nanodomain morphology further dictates material properties based on state-of-the-art literature examples.

Macro- Versus Microphase Separation Behavior

Block copolymers are capable of microphase separation on nanometer length scales into well-defined ordered nanophases both in the undiluted state and in blends (Matsen and Bates 1996; Bates and Fredrickson 1999). These morphologies are determined mainly due to the balance between enthalpic penalty arising from association between different blocks and the restrictions imposed by covalent bonds linking blocks. Block copolymer morphologies are dictated by polymer length, block symmetry, and interblock repulsion strength. Furthermore, when BCP are blended with homopolymers and copolymers or are in solution, other parameters as solvent-block interaction parameters and blend composition further determine block copolymer morphology.

Phase behavior of epoxy/BCP blends can be roughly modeled by considering each system as a solution of a BCP in a block-selective solvent (epoxy precursors) which evolves during the curing process, through a BCP/block-selective polymer blend, into a cross-linked epoxy network bearing BCP-separated domains.

There are two possible scenarios when blending block copolymer with epoxy precursors: (a) *microphase-separated system*, where the block copolymer induces nanodomain inclusions within the epoxy matrix, and (b) *macrophase-separated system* consisting of a multiphase system with a well-defined epoxy phase and block copolymer-rich phase in the submicron length scale.

A simple and approximate approach to anticipate whether micro- or macrophase separation will take place for a given epoxy/BCP blend is by direct comparison between solubility parameters (δ) of each block and those for the epoxy precursors, which can be considered as reactive solvents before curing.

The solubility between a polymer and a solvent is determined by the polymer-solvent interaction parameter $\chi_{\text{polymer-solvent}}$, defined by Eq. 1:

$$\chi_{\text{polymer-solvent}} = \frac{Z\chi_{\text{polymer}} \Delta w_{\text{polymer-solvent}}}{k_B T} = \chi_H + \chi_S \quad (1)$$

Here, Z is the lattice coordination number, χ_{polymer} is the number of polymer segments per solvent molecule (usually assumed as one), $\Delta w_{\text{polymer-solvent}}$ is the interaction free energy associated with the formation of an unlike contact pair between segments of a solvent and a polymer molecule, k_B is the Boltzmann constant, and $k_B T$ is the thermal energy. $\chi_{\text{polymer-solvent}}$ is expressed in terms of an enthalpic, χ_H , and an entropic contribution, χ_S . The enthalpic component χ_H can be calculated in terms of the solubility parameters as by Eq. 2:

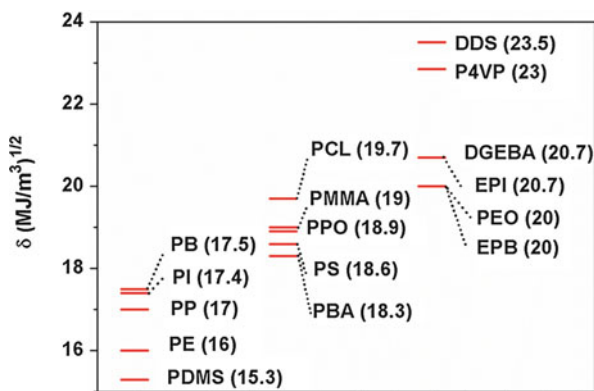
$$\chi_H = \frac{V_{\text{solvent}}}{RT} \left((\delta_{\text{polymer}} - \delta_{\text{solvent}})^2 + 2I_{\text{polymer-solvent}} \delta_{\text{polymer}} \delta_{\text{solvent}} \right) \approx \frac{V_1 (\delta_{\text{polymer}} - \delta_{\text{solvent}})^2}{RT} \tag{2}$$

where V_{solvent} is the solvent molar volume; R is the gas constant; δ_{polymer} and δ_{solvent} are the solubility parameters of polymer and solvent, respectively; and I is a binary parameter between solvent and polymer, which can be approximated to a zero value (Mikos and Peppas 1988).

Therefore, those polymer-solvent systems with similar δ values tend to be miscible with one another ($\delta_{\text{polymer}} - \delta_{\text{solvent}} \rightarrow \text{zero}$). Solubility parameters (δ) for selected polymers diglycidyl ether of bisphenol A (DGEBA) and hardener are given in Fig. 1.

Following the previous analysis, it can be anticipated that interactions between ePI ($\delta_{\text{ePI}} = 20.7 \text{ (MJ/m}^3)^{1/2}$) and epoxy monomer DGEBA ($\delta_{\text{DGEBA}} = 20.7 \text{ (MJ/m}^3)^{1/2}$) are favorable enough to enable miscibility. Grubbs et al. (2000) calculated the solubility parameters for epoxidized polyisoprene of poly(butadiene-*b*-isoprene-*ran*-epoxidizedisoprene) with epoxidation degrees of 75% and 46%. By doing so, it was determined that interactions between epoxidated BCP in 75% and epoxy precursors are favorable enough to enable miscibility of these highly epoxidized systems, while at lower epoxidation degree (46%), the interactions between BCP and the epoxy component are sufficiently unfavorable. Since polybutadiene block is also immiscible with the epoxy precursors, macrophase separation occurs for the BCP with epoxidation degree of 46%.

Fig. 1 Solubility parameter for different polymers and epoxy precursors (Barton 1990; Van Krevelen 1990; Ng and Chee 1997; Yu et al. 1997; Bordes et al. 2010; O’Driscoll et al. 2011)

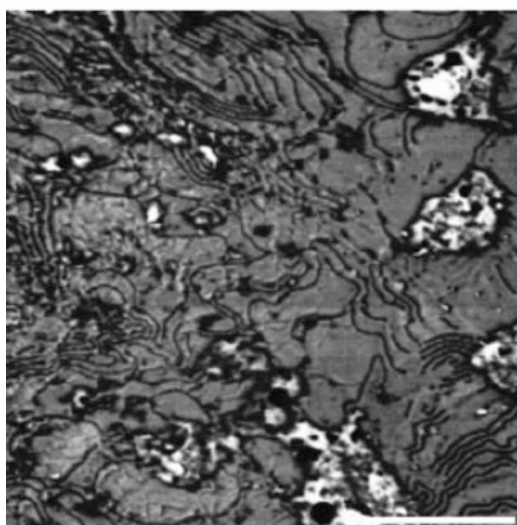


Macrophase-separated epoxy/BCP blends are characterized by opaque aspect due to light scattering of separated domains with dimensions comparable to the wavelength of visible light. On the contrary, the nanometer length domain size in microphase-separated systems avoids this effect, and therefore such materials are transparent. For this reason, a practical and simple strategy to anticipate whether micro- or macrophase separation occurs is by direct inspection of the system or by optical microscopy. Macrophase-separated systems are composed by separated epoxy-rich phase and copolymer-rich phase with domain lengths on the order of several hundred nanometers. These copolymer-rich domains are almost pure copolymer regions that involve separate compartments of ordered features similar to those encountered in the corresponding parent copolymer, as shown in Fig. 2 for an immiscible epoxy/poly(styrene-*b*-butadiene) blend (Serrano et al. 2004).

As the cure process begins, the molecular weight of the growing epoxy matrix diverges, and the correspondingly large increase in the copolymer degree of polymerization N overcomes the favorable interaction parameter value and drives χN (the strength of interblock repulsion), where χ is the Flory-Huggins interaction parameter, to values large enough to exceed critical phase separation condition and therefore promotes phase separation.

Following this analysis, it might be thought that the final system after curing epoxy/BCP blends should always be macrophase separated, as for the case of traditional epoxy/homopolymer blends. However, this is not the case because the highly cross-linked epoxy network substantially reduces chain mobility of the copolymer, and therefore the tendency toward macrophase separation is greatly retarded, as the cure process progresses. This kinetic restriction due to the increase in molecular weight and cross-linking avoids the possibility of coarsening and growth of phase-separated domains and is responsible for the evolution of the epoxy/BCP blends to a microphase-separated state. Therefore, both thermodynamic

Fig. 2 TEM micrograph of macrophase-separated epoxy/poly(styrene-*b*-butadiene) blend. Scale bar = 1 μm (Reprinted with permission from Serrano et al. (2004). Copyright (2004). John Wiley and Sons)



and kinetic effects compete during the cure process of epoxy/BCP blends as manifested in the phase behavior of partially epoxidized poly(styrene-*b*-butadiene) (SB) within epoxy system studied by Serrano et al. (2007). Epoxidized SB block copolymers with epoxidation degree in the range of 37–46% are suitable candidates to understand the phase behavior of epoxy/BCP blends, since the incorporation of oxirane ring to the immiscible polybutadiene block gives access to BCP with tuned miscibility with epoxy precursors. In this regard the epoxidized block of SB with an epoxidation degree of 37% (SB37) and 46% (SB46) are both initially miscible with the epoxy precursors, but epoxidized polybutadiene block of SB46 is more miscible than the corresponding epoxidized block of SB37 due to a similar solubility parameter with the epoxy precursors. Transmission electron microscopy (TEM) images of cured epoxy/SB37 and epoxy/SB46 showed the nanostructured pattern of both systems. Epoxy/SB37 presented a combination of spherical and wormlike structures, while epoxy/SB46 system consisted of ordered spherical micelles, as presented in Fig. 3. These morphological differences suggest that the epoxybutadiene blocks with epoxidation degrees of 37% are only barely miscible with the uncured epoxy resin. As the molecular weight of the epoxy resin increases during cure, the miscibility between epoxy resin and epoxybutadiene block decreases to the point where phase separation begins at much lower conversions than for the case of highly epoxidized epoxybutadiene block of SB46. When phase separation begins at this lower conversion, the viscosity of the growing epoxy network is low enough to allow nucleation and growth of block copolymer domains, allowing the shift from spherical micelles to aggregated micelles in the form of wormlike structures. On the contrary, growth of phase-separated domains in epoxy/SB46 blends is arrested because the gelation of the curing resin occurs at a

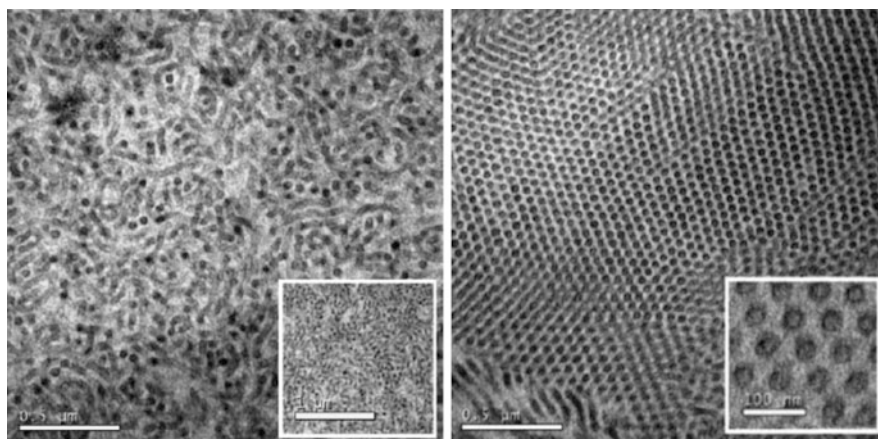
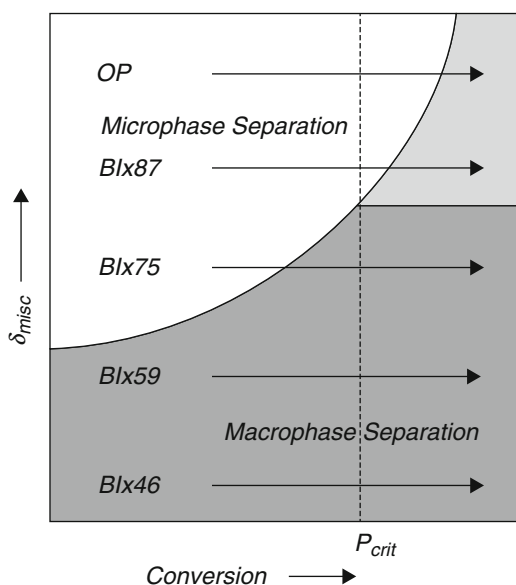


Fig. 3 TEM micrographs of microphase-separated epoxy/partially epoxidized poly(styrene-*b*-butadiene) blend. The epoxidation degree is 37% (*left*) and 46% (*right*). Scale bars = 0.5 μm. Scale bars in the inset = 1 μm (*left*) and 100 nm (*right*) (Reprinted with permission from Serrano et al. (2007). Copyright (2007). John Wiley and Sons)

similar curing conversion or prior to the critical segregation limit χN_{crit} . Since χ is related with the segregation strength, being lower for epoxy/epoxypolybutadiene 46 than the corresponding parameter for epoxy/epoxypolybutadiene 37, the product χN overcomes critical phase separation limit χN_{crit} at lower N , or lower epoxy conversion for SB37 than for SB46.

In this regard, Grubbs et al. (2000) synthesized poly(butadiene-*b*-isoprene) (BI) block copolymers selectively epoxidized in the isoprene units (BIe) with epoxidation degrees ranging from 46% to 87%, in order to classify each epoxy/BCP blend according to their phase separation behavior (micro- or macrophase separation) as a function of miscibility and epoxy conversion. As a result of their analysis, the authors proposed a phase separation behavior map, which is shown in Fig. 4 and contains valuable information on how a given epoxy/BIE blend evolves during curing. Dark gray regions in the map correspond to macrophase-separated systems. For instance, the epoxidation degree of BI46 is low enough to prevent miscibility from the initial uncured system, and therefore it is situated in the macrophase-separated region, regardless of the epoxy conversion. For the case of BI75, the initial epoxy/BCP blend is miscible, and it situates in the microphase separation region (white region). However, as the polymerization reaction proceeds, the system evolves to the macrophase separation region (dark gray) before reaching the critical epoxy conversion (p_{crit}), after which the system is kinetically hindered to phase separate. On the contrary, by further increasing initial miscibility between epoxidized polyisoprene blocks and epoxy precursors, epoxy/BI87 blend surpasses the critical epoxy conversion in the microphase-separated region (white), indicating that the final material is nanostructured. It is worth noting that if the epoxy conversion is further increased, the system should situate in the macrophase-separated region as the product $\chi N > \chi N_{crit}$.

Fig. 4 Proposed mapping of phase separation in epoxy/BCP blends as a function of miscibility and epoxy conversion (Reprinted with permission from Grubbs et al. (2000). Copyright (2000). American Chemical Society)



This thermodynamically stable region is however not accessible due to the increased viscosity of the cross-linked system as the epoxy conversion exceeds p_{crit} , which fixes the material in the microphase-separated state as indicated by light gray color. A similar scenario occurs for the more miscible epoxy/poly(ethylene oxide-*b*-ethylene-*alt*-propylene) (OP) blend.

While the absence of macrophase separation in epoxy/BCP blend systems is the result of both thermodynamic and kinetic factors, not all microphase-separated epoxy/BCP systems are obtained by the same sequence of events. The following section describes the possible operating mechanisms that lead to epoxy/BCP nanostructured systems, as well as practical considerations to follow and determine which mechanism occurs and the key parameters affecting nanostructured systems.

Microphase Separation Mechanisms

Blends between BCP and epoxy precursors can be considered as a special case of microphase separation of BCP in solution (Grubbs et al. 2000; Ritzenthaler et al. 2002; Maiez-Tribut et al. 2007). General procedures to obtain nanostructured epoxy/BCP systems involve the use of solvents, and in many cases the epoxy precursors can be considered as reactive solvents in the uncured state. In this section it will be discussed how the interplay between each block of the selected BCP and the epoxy precursors play a key role in the evolution of the nanostructuring mechanisms. Fully characterization of the actual sequence of events by which a given epoxy/BCP blend microphase separates is of great interest because it has significant impact not only in the final morphological pattern displayed by the material, but also and more importantly in the material properties.

The sequence of events by which block copolymers microphase separate within epoxy systems can be classified by two major mechanisms:

1. Polymerization-induced microphase separation
2. Self-assembly

The main difference between both general mechanisms is the initial thermodynamic condition in the uncured state which dictates the epoxy conversion at which the nanoscopic objects are formed.

The polymerization-induced microphase separation (PIMPS) mechanism consists of an initially miscible epoxy/BCP precursor blend which evolves to a nanostructured system in the course of the epoxy precursor polymerization. On the other hand, if an epoxy/BCP blend follows a self-assembly (SA) mechanism, there is at least one block that is not miscible with the epoxy precursors in the uncured state and at least one block which is miscible with the epoxy precursors. The immiscible block self-assembles due to the enthalpic energy contribution gained by contacts of identical subchains which overcomes the mixing entropy of the nonsegregated system. SA mechanism consists of an initially preformed nanostructure that is subsequently fixed by network formation.

Although there are many epoxy/BCP systems whose nanostructure formation can be explained by these proposed mechanisms, many others are quite more complicated and cannot be interpreted by simply considering isolated SA or PIMPS mechanisms. In fact, it is possible that the actual mechanism taking place in the formation of nanostructured epoxy/BCP blends corresponds to a “tandem-like” sequence which combines more than one mechanism, such as SA, followed by PIMPS, or PIMPS followed by a second PIMPS.

In this section, a detailed description of each basic mechanism will be given, as well as examples following “tandem-like” mechanisms.

The introduction of solvents increases the level of complexity to understand microphase separation of BCP with epoxy systems. For example, the microphase separation of a general AB block copolymer in a mixture of epoxy monomer (em) and hardener (h) involves six χ parameters: χ_{AB} , χ_{A-em} , χ_{A-h} , χ_{B-em} , χ_{B-h} , and χ_{em-h} . Of course that by increasing the number of blocks of the BCP or using more solvents in the formulation, the complexity of the BCP self-assembly further increases. For simplicity, but without loss of generality, in this section the discussion will be focused on the possible microphase separation mechanisms for a system composed by AB block copolymer, epoxy monomer and hardener.

Depending on the solubility of the blocks in the epoxy monomer and hardener at the curing conditions, the block copolymer AB can be characterized into amphiphilic with one epoxy-philic segment and one epoxy-phobic segment, double “epoxy-philic” or double “epoxy-phobic.” Of course double “epoxy-phobic” BCP are not the subject of the present section as they will macrophase separate due to the lack of miscibility of both blocks with the epoxy precursors, as already discussed in the previous section. Therefore, herein we will focus on amphiphilic BCP and double “epoxy-philic” AB BCP (Amendt et al. 2012; May and Eisenberg 2012).

Nanostructuring mechanism for BCP bearing at least one “epoxy-phobic” block starts before curing and proceeds during curing, while BCP with block solubility parameters very similar to those for the epoxy precursors undergo microphase separation only during curing and thus will be discussed first.

Microphase Separation During Curing

Epoxy/BCP blend nanostructure can be formed in situ during the curing reaction when all blocks are miscible with the epoxy precursors in the uncured state. For diblock copolymers, this situation occurs for “double epoxy-philic” BCP at the curing condition temperature. Although there might be not many BCP completely miscible with an epoxy system at room temperature, it is well known that many epoxy system/homopolymer blends (PS, PMMA, epoxidized polybutadiene, among others) display upper critical solution temperature (UCST), above which the epoxy/polymer blend is miscible (homogeneous phase). Therefore, if the curing temperature for a given epoxy/BCP blend is above the UCST, then such system meets the initial conditions. At epoxy conversion 0% these systems are homogeneous, and no phase-separated domains are formed (stable system, ΔG mixing < 0). During the

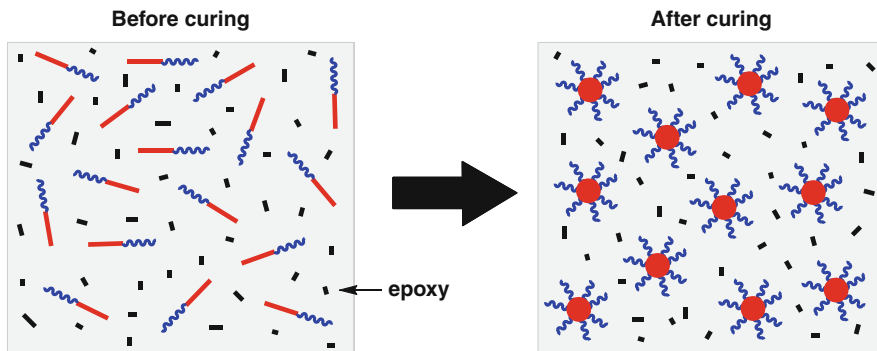


Fig. 5 Schematic of the development of nanoscopic structures by PIMPS in epoxy/BCP blends

course of the polymerization, there are thermodynamic factors which drive microphase separation of the BCP (Fig. 5). Such mechanism is called *polymerization-induced microphase separation* and is a particular case of the more general reaction-induced phase separation (RIPS) mechanism, where the chemical reaction taking place is the polymerization of the epoxy precursors (i.e., epoxy/amine polycondensation). The RIPS mechanism is well known to occur in thermosetting blends containing homopolymers (and/or random copolymers) where structures of the order of magnitude of micrometers in size can be formed via spinodal decomposition and/or nucleation and growth mechanism. A vast literature is available in the field of rubber-modified epoxies (Verchère et al. 1989; Chen et al. 1994; Williams et al. 1997).

Events involved in microphase separation induced by polymerization process are determined by thermodynamic and kinetic factors. A thermodynamic analysis enables to determine the regions where the system is stable (no phase separation occurs), metastable (phase separation may occur), or unstable (phase separation takes place). The following thermodynamic analysis proposed by Williams et al. (Williams et al. 1997) is based on a Flory-Huggins model and is valid for a monodisperse constituent. This is a simple approach that serves to get a qualitative insight into the reaction-induced microphase separation in the pregel stage.

In this model the entropy of mixing per unit volume is given by Eq. 3:

$$\Delta S = -R \left(\frac{\phi_P}{V_P} \ln \phi_P + \frac{\phi_M}{V_M} \ln \phi_M \right) \quad (3)$$

where R is the gas constant, ϕ_P is the volume fraction for the epoxy thermoset, ϕ_M is the volume fraction of the miscible block, and V_i is the molar volume of component i in the mixture. Here, $\phi_P + \phi_M = 1$.

The enthalpy of mixing per unit volume is given by Eq. 4:

$$\Delta H = \left(\frac{RT}{V_r} \right) \chi \phi_P \phi_M \quad (4)$$

where χ is the Flory-Huggins interaction parameter between the epoxy and the block under consideration and V_r is the volume of the unit cell usually referred to as the reference volume.

This leads to a Gibbs free energy per unit volume given by Eq. 5:

$$\Delta G = \Delta H - T\Delta S = \left(\frac{RT}{V_r}\right) \left(\frac{\phi_P}{V_P/V_r} \ln\phi_P + \frac{\phi_M}{V_M/V_r} \ln\phi_M + \chi\phi_P\phi_M \right) \quad (5)$$

At this point two important considerations must be highlighted.

First, during the curing reaction, the ratio V_P/V_r increases as the volume of the thermosetting polymer increases. On the other hand, the ratio V_M/V_r is constant. Therefore, the entropic contribution to the free energy of mixing decreases during polymerization. In particular, at the gel point, where the viscosity of the system and the molecular weight of the polymer network diverge, the entropic contribution is minimal. Therefore, this aspect highlights the chain growth effect on the free energy of mixing. A second important contribution to the free energy is that, as the curing reaction progresses, the conversion of oxirane rings of the epoxy precursor is transformed to more polar functional groups. For example, when the used hardener is a diamine, the obtained β -aminoalcohols are more polar than the epoxide precursors. By this transformation, the epoxy/block copolymer interaction parameter χ increases in the course of the polymerization, contributing positively to the free energy enthalpic term.

It is possible to anticipate that the above factors may cause the system to cross thermodynamic phase boundaries and result in a transition from an initial homogeneous state to a microphase-separated state. In the case of the thermosets containing block copolymers, the surface tension of domains of phase-separated blocks is reduced by the presence of the miscible block within the epoxy system giving rise to phase separation at the nanoscale (microphase separation).

In order to achieve nanostructured epoxy/BCP systems by PIMPS, it might be of great importance to select a proper combination of blocks and epoxy precursors so that the critical phase separation occurs before gelation for one block and after the gel point for the other block (high conversion). If the critical phase separation of both blocks occurs at a similar conversion, it might be possible to produce simultaneous PIMPS of both blocks that lead to a macrophase-separated state.

Apart from the thermodynamic factors that dictate phase separation in epoxy/BCP blends during the course of the reaction, it is also very important to consider kinetic aspects of this process. The possibility to achieve nanostructured systems is also governed by the competition between the phase separation rate (k_{psep}) and the polymerization rate (k_{pol}). Let's consider a system that crosses the thermodynamic boundaries in the pregel stage where the k_{psep} tends to be infinite and k_{pol} is near zero. Under these conditions, phase separation will occur instantly with no considerable increase in the conversion. At this point, if the phase-separated domains have enough time to coarsen and grow, they could even lead to undesirable aggregated domains and shift in the morphological pattern. If the opposite scenario

takes place (k_{pol} tends to be infinite and k_{psep} near zero), phase separation process may have not enough time to occur, and the immiscible block may remain trapped within the growing cross-linked network, precluding a nanostructured system. In real systems, the actual behavior might be in the middle of these extreme conditions. For instance, Fan et al. reported a partially demixing process of poly(ϵ -caprolactone) (PCL) block of polystyrene-*block*-poly(ϵ -caprolactone)-*block*-poly(*n*-butyl acrylate) based on glass transition temperature analysis of the nanostructured materials (Fan et al. 2010). Typical variables that can be adjusted to tune the rate k_{pol} and k_{psep} will be discussed in the next section (Fig. 5).

In summary, the driving forces governing PIMPS mechanism in epoxy/BCP blends are attributed to the following aspects:

- The increased molecular weight owing to polymerization (curing reaction), which gives rise to the decreased contribution of mixing entropy to the free energy of mixing
- The typical increase of the intercomponent interaction parameters (χ) with epoxy conversion
- Competitive kinetics of curing reaction and microphase separation

It should be mentioned that the effect of the increased molecular weight is much more significant than any change produced in the interaction parameter due to modification of chemical structures (Williams et al. 1997).

Microphase Separation Before Curing

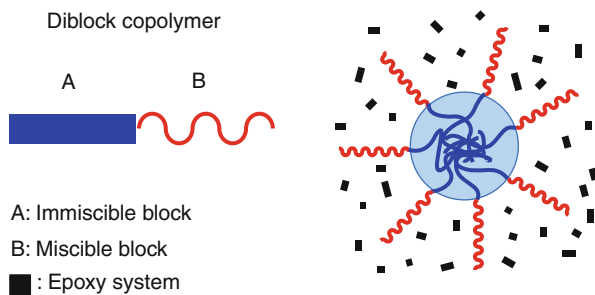
First Step: Morphologies Initiated by Self-Assembly

Self-assembly (SA) is one of the most studied microphase separation mechanisms for epoxy/BCP blends (Hillmyer et al. 1997, Xu and Zheng 2007). BCP following this type of mechanism are generally amphiphilic BCP, since the condition for SA is that at least one block is miscible with the epoxy and at least one block is immiscible in the uncured epoxy precursors. Under these conditions, the initial self-assembly process of the immiscible block is driven by the unfavorable mixing enthalpy coupled with a small mixing entropy, with the covalent bond connecting the blocks preventing macroscopic phase separation. The immiscible block self-assembles into a wide range of morphologies such as spheres, cylinders, wormlike, and lamellae, among others, depending on different formulation characteristics which will be discussed in the following section. The epoxy-miscible B block subchains extend from the A-B interface to the epoxy-rich region in a brushlike configuration as pictured in Fig. 6.

Second Step: Immobilization by Polymerization

The SA mechanism is followed by a stabilization step in which the aggregated nanostructures are immobilized by network formation during the epoxy curing

Fig. 6 Self-assembly of AB diblock copolymer. Self-assembled A blocks into spherical domains and B blocks in a brush-like configuration



process. This step is absolutely important to preserve the initially obtained nanostructure.

In order to highlight the relevance of this step in the mechanism, it can be useful to compare the following two hypothetical systems:

1. Amphiphilic AB block copolymer blended with the epoxy precursors that act as selective solvents for B before (*state a*) and after curing (*state b*)
2. Amphiphilic AB block copolymer with a selective solvent for B block (*state a*), which is gradually replaced by a more polar solvent (*state b*)

In the corresponding *state a* for both systems, it is expected that A subchains form aggregates by self-assembly in both systems, due to the amphiphilic nature of AB block copolymer. In the *b state* for both systems, there will be an increase in the product $\chi N_{\text{B-epoxy}}$ once the curing reaction begins in system 1 and an increase in product $\chi N_{\text{B-solvent}}$ for system 2, as the polarity of the solvent increases. Although the initial self-assembly and the subsequent increase in χN may anticipate a similar phase behavior for both systems in *state b*, they will actually behave completely different. System 1 will evolve to a microphase-separated material, while system 2 will end up in a macroscopically separated system (polymer and solvent). The reason for this difference, even when the thermodynamic may seem to be very similar, is that in system 1, the viscosity increases with the polymerization reaction and this reduces chain mobility and domain growth mechanism. Therefore, the size of the BCP domains are limited to the nanoscale, as determined by the initial self-assembly. On the other hand, in system 2 the initial nanodomains have no restriction to move and grow and will finally end up in the micrometric length scale.

Although the previous systems are hypothetical, they are helpful to get an approximate picture of the importance of the BCP chain immobilization process given by the epoxy/hardener polymerization during curing.

“Tandem-Like” Mechanisms

The preservation of the morphologies obtained by PIMPS or SA mechanisms requires that the block copolymer entering in the composition has to be compatible

with the matrix at any stage of the curing. Since the chemical nature of the material is varying with time during curing, a block copolymer selected for a given curable composition may become completely inappropriate once curing is completed. In practice, this condition is hardly reached, and therefore there are additional steps occurring after PIMPS or SA mechanisms, which are generally a combination of these mechanisms. Thus, the whole sequence of events operating in the nanostructuration process will be referred to as “tandem-like” mechanisms.

Self-Assembly Followed by Immobilization by Polymerization + Demixing

This combined mechanism is generally the case for amphiphilic block copolymers that first self-assemble into ordered morphologies, but in the course of the curing process, the miscible block undergoes a demixing process based on the PIMPS mechanism. For instance, Lipic et al. studied blends of poly(ethylene oxide)-poly(ethylene-*alt*-propylene) (PEO-PEP) diblock copolymer with an epoxy system (BPA348/MDA) and tracked the evolution of morphology during the cross-linking by means of small angle X-ray spectroscopy (SAXS) (Lipic et al. 1998). The authors found that in the uncured state the sample presented a cylindrical morphology which was retained during curing (SA followed by immobilization by reaction). However, SAXS measurements evidenced an increase in the principal spacing (d^*) of around 15% as the epoxy cures, as pictured in Fig. 7.

Of course the final morphology cannot be explained only by SA followed by immobilization, and therefore the actual mechanism operating in this system is likely to be a combination of SA followed by immobilization and a local expulsion of the initially miscible PEO blocks by PIMPS mechanism.

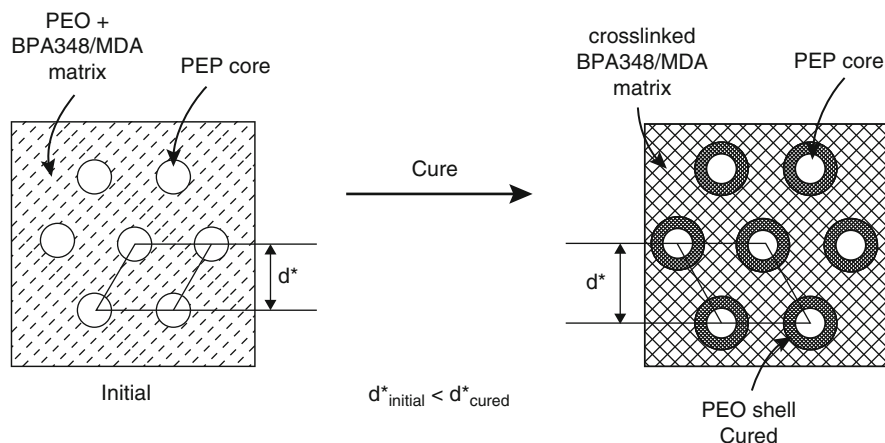


Fig. 7 Structural changes that accompany curing of an epoxy/OP system blend with a hexagonally packed cylindrical microstructure. Cross-linking the epoxy resin leads to a core and shell structure and an increase in the principal spacing d^* (Reprinted with permission from Lipic et al. (1998). Copyright (1998). American Chemical Society)

Self-Assembly Followed by Immobilization by Polymerization + Reaction

Gelation of the epoxy matrix is effective to attain a microphase-separated material, but as detailed in the previous mechanism, maintaining the same nanodomain dimensions and morphology than that for the initially uncured state is almost impossible because the initially miscible block cannot be miscible with the growing thermoset throughout the entire curing cycle. In this regard, Grubbs et al. (2000) implemented a different approach by incorporating functional groups into the block copolymer capable of reacting with the amine end group of the hardener so that the block copolymer could cure within the epoxy network without phase separation. In a subsequent work by Rebizant et al. (2004), the authors showed that it is possible to use any functional group, preferably located in the structuring block and able to react with epoxy, amine groups, or both of them. By doing so, these authors introduced the concept of reactive block copolymers, which are BCP bearing miscible blocks capable to react in a competitive way toward the epoxy precursors during curing. Figure 8 shows TEM images of a poly(styrene-*b*-butadiene-*b*-methyl methacrylate-*b*-glycidyl methacrylate) (SBMG) BCP blended with DGEBA and 4,4'-diaminodiphenylsulfone (DDS) as epoxy precursors before (a) and after

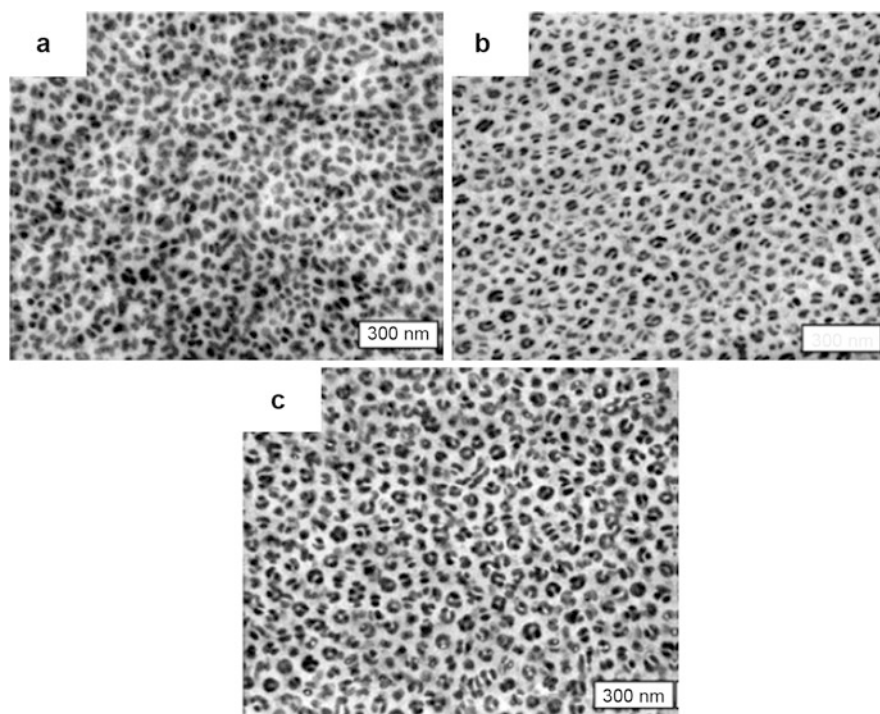


Fig. 8 TEM micrographs of DGEBA/DDS blends with 30 wt.% of (a) SBMG before curing, (b) SBMG after curing 5 h at 135 °C, and (c) SBMG after curing 5 h at 220 °C. Scale bar = 300 nm (Reprinted with permission from Rebizant et al. (2003). Copyright (2003). American Chemical Society)

(b) curing (Rebizant et al. 2003). In this system, oxirane groups of glycidyl methacrylate block are capable to react with the DDS at a similar rate than that for the DGEBA/DDS reaction.

The initial nanostructured pattern before curing was characterized by a raspberry-like morphology with dark spheres of polybutadiene on light spheres of polystyrene within DGEBA-DDS prepolymer mixture (Fig. 8a). After curing the system under different conditions, it was observed that the morphology was retained almost unchanged, whatever the curing temperature. In particular, the size of included objects remained smaller than 70 nm, in agreement with the visual aspect of the films.

Grubbs et al. (2000) proposed three possible curing scenarios for epoxy/BCP blends following initial self-assembly, which are summarized in Fig. 9. If the epoxy-miscible block is not reactive toward the epoxy precursors, it undergoes local expulsion from the epoxy network to the surrounding self-assembled nanodomain during curing (Fig. 9a). On the contrary, the incorporation of reactive functional groups in the BCP avoids local expulsion if the reaction epoxy precursor/BCP competes against the reaction between the epoxy precursors (Fig. 9b) or undergoes local expulsion followed by interfacial reaction if the reactivity of the BCP against the epoxy precursor is lower than that for epoxy/hardener (Fig. 9c).

Multiple Polymerization-Induced Microphase Separation

The nanostructuring mechanisms of epoxy/BCP blends bearing three or more blocks are much richer than that for the corresponding two-component diblocks or triblocks because multiple interaction parameters ($\chi_{\text{block } i\text{-epoxy}}$) result from the presence of more than two-component BCP. In this regard, the mechanistic studies reported by Fan et al. (2010) about the microphase separation behavior of epoxy/ABC BCP blend are of particular interest. The authors used a polystyrene-*block*-poly(ϵ -caprolactone)-*block*-poly(*n*-butyl acrylate) (PS-PCL-PBA) ABC triblock

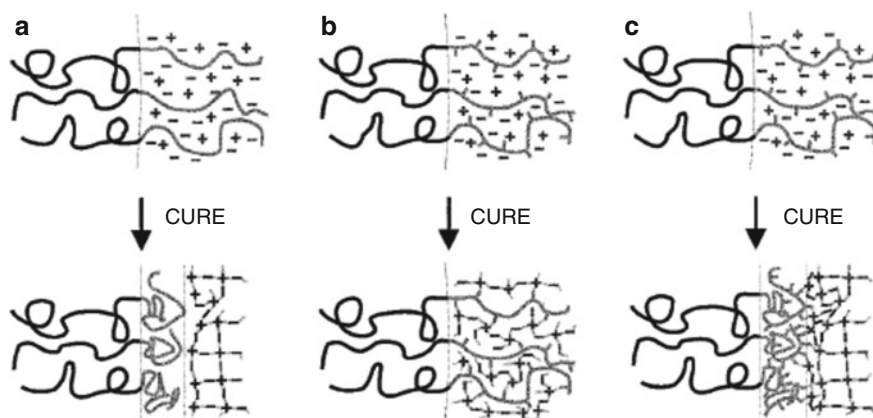


Fig. 9 Comparison of microphase separation process during cure of nonreactive BCP (a) and reactive copolymer: copolymer cures within epoxy matrix (b) or copolymer cures interfacially after expulsion from epoxy phase (c) (Reprinted with permission from Grubbs et al. (2000). Copyright (2000). American Chemical Society)

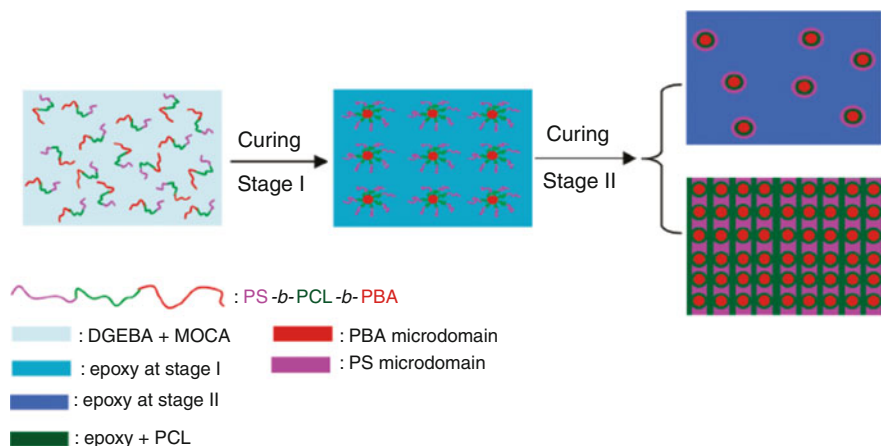


Fig. 10 Double reaction-induced microphase separation in thermosetting blends of epoxy with PS-*b*-PCL-*b*-PBA triblock copolymer

copolymer, where the three blocks were initially miscible in the epoxy precursors. By employing epoxy/PS and epoxy/PBA binary models, it was determined that the phase separation of PBA subchains occurred before than the PS subchains during the curing reaction. Moreover, the preformed PBA nanophases could act as the template of the polymerization-induced microphase separation of PS subchains and confine PS block nanophases around the PBA nanodomains. The sequential demixing of PBA and PS subchains resulted from the higher intermolecular interaction parameter for epoxy/PBA than for epoxy/PS. Figure 10 depicts the multicomponent morphologies that can be obtained by multiple PIMPS mechanisms (Fan et al. 2010). Recent studies by Yu et al. (Yu and Zheng 2011) on epoxy/BCP blends using a PS-*b*-PCL-*b*-PEO block copolymer and DDS as hardener described a similar microphase separation mechanism consisting of double polymerization-induced microphase separation of PS subchains followed by PCL subchain demixing.

In this context, the actual mechanism operating for epoxy/BCP blends, where the BCP contains more than two components, can be a combination of simpler mechanisms occurring in a sequential or simultaneous fashion. By taking these considerations into account, the complexity of the obtained morphologies highly increases with the number of blocks.

Experimental Strategies to Follow Microphase Separation Mechanism

The most convenient way to establish if a phase separation mechanism occurs by PIMPS is to use different experimental techniques giving different size scales of the generated morphology, i.e., SAXS, and to observe the evolution of morphologies by scanning electron microscopy (SEM), TEM, or atomic force microscopy (AFM) at the

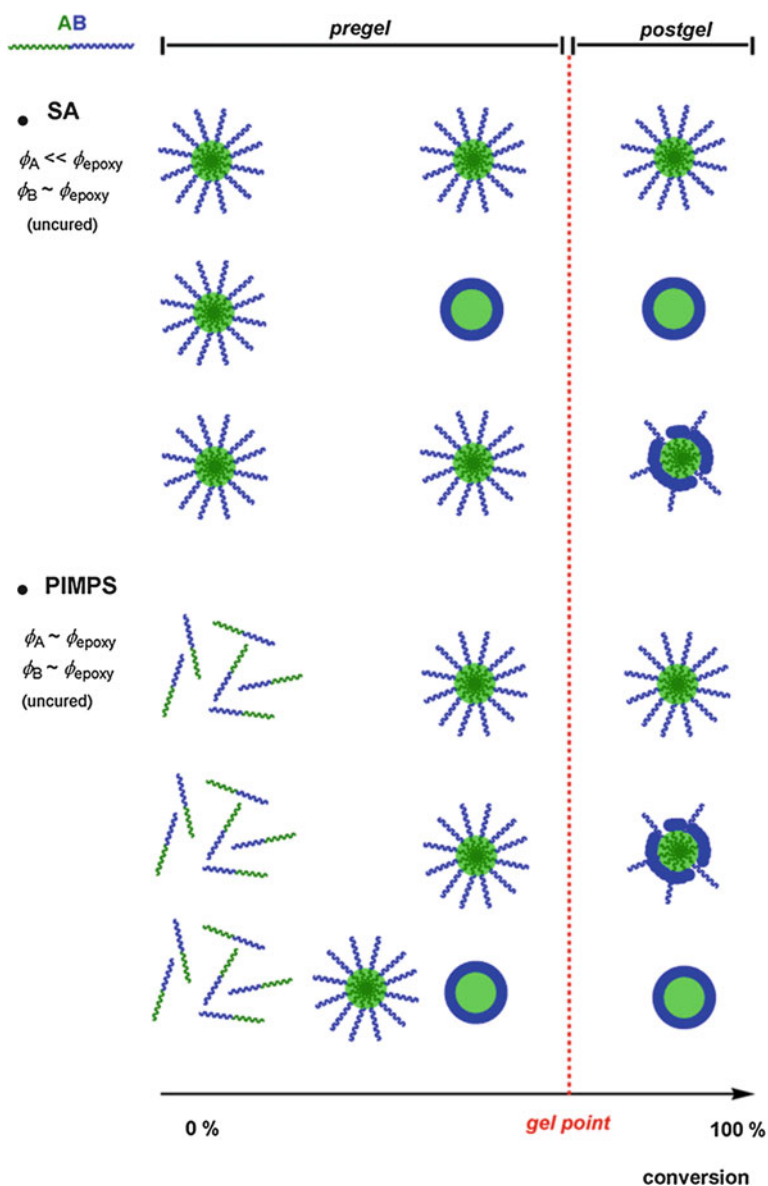


Fig. 11 Schematic representation of the possible sequence of events occurring during microphase separation of AB diblock copolymers within epoxy systems depending on block and epoxy precursors solubility parameters as a function of epoxy conversion

same curing times as SAXS and light scattering (LS) observations (Lipic et al. 1998; Mijovic et al. 2000; Fan and Zheng 2008; Hu and Zheng 2009). Figure 11 summarizes the possible sequence of events occurring during microphase separation of AB diblock copolymers within epoxy systems as a function of the epoxy conversion.

Key Parameters Affecting Mechanisms and Morphologies

This section explores more in detail the underlying factors controlling the morphology of epoxy/BCP blends in both the unreacted and the reacted states.

Epoxy/BCP Composition

One of the main parameters that determines the morphology in epoxy/BCP blends is the overall blend composition (ϕ) expressed in terms of epoxy precursors of block copolymer.

Let's consider a symmetric AB diblock copolymer, where A block is immiscible in the epoxy precursors and B block is fully miscible. The progression of morphologies can be rationalized by considering B subchains as brushes extending from A to B interface. B block exists as a "dry" brush in the neat block copolymer (lamellar morphology), leading to an interfacial curvature controlled by the block symmetry.

The incorporation of epoxy monomers in the uncured state (0% epoxy conversion) results in selective solubilization of the epoxy monomers in the B domains producing a swollen "wet" B brush, leading to an increased volume per B subchain, while the volume per A subchain remains constant. If the value of $\phi_{\text{epoxy monomers}}$ is increased, then the epoxy monomers may ultimately change the packing arrangement of chains along the interface and consequently induce a change in the interfacial curvature. In the swollen state, the lamellar morphology cannot support interfacial curvature, and therefore, the system shifts to the gyroid, cylinder, and spherical morphologies as the amount $\phi_{\text{epoxy monomers}}$ is increased (Fig. 12).

By doing so, it is then possible to effect a transition from one morphology to another by varying the epoxy monomer fraction in the epoxy/BCP blend. Figure 13 presents a composition-conversion diagram showing changes in morphology for epoxy/PEP-*b*-PEO blends proposed by Lipic et al. (1998). Phase behavior in the uncured state corresponds well with the behavior predicted and observed for blends of block copolymers with a solvent selective for one block, with a progression of morphologies from lamellar to G, C, and S as the epoxy monomer content

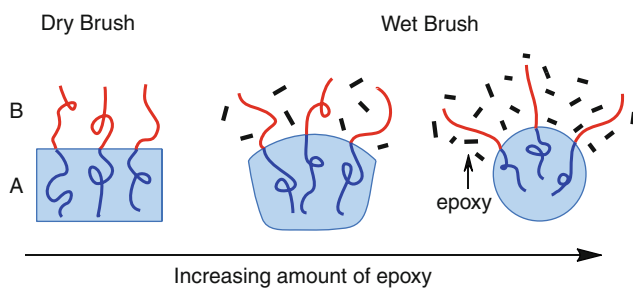
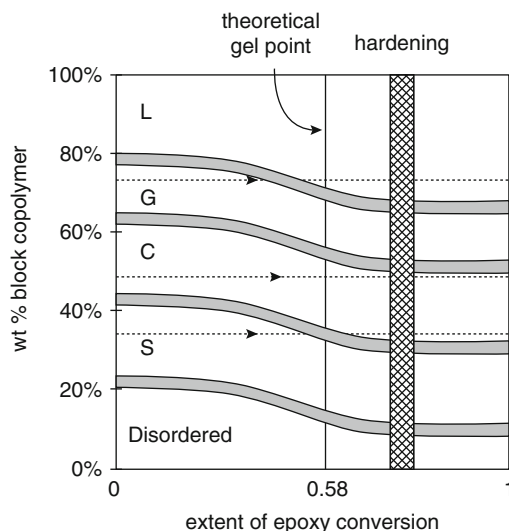


Fig. 12 Illustration of swelling-induced change in the interfacial curvature for epoxy/A-B (epoxy selective) blends

Fig. 13 Proposed composition-conversion diagram showing changes in morphology with cure. The two-phase coexistence windows are shaded, and the dotted lines indicate the path taken by certain conditions. At high degrees of epoxy conversion, the tightly cross-linked matrix prevents further changes in the morphology, and the phase boundaries no longer shift (Adapted with permission from Lipic et al. (1998). Copyright (1998). American Chemical Society)



increases. During curing at a constant BCP%, indicated by the trajectories of dotted lines, PEO blocks are demixed by the growing of epoxy network, as discussed in the previous section. This creates conformational strain which induces order-order phase transitions to the “dry brush” (gyroid (G) to lamellar (L), cylinder (C) to G, and spherical (S) to C), as the nanostructured epoxy network forms.

Number of Block Types

One of the principal molecular variables that influences BCP microphase separation within an epoxy system is the number of block types. Obviously, by increasing the number of block types, the number of events increases too and so does the complexity of the nanostructuring mechanism.

BCP with two different blocks (AB and ABA) typically can adopt four different nanodomain morphologies (lamellae, gyroid, cylinders, and spheres) when blended with epoxy systems. Introduction of a third block type (ABC) expands the spectrum of possible nanostructured morphologies. Figure 14 shows different nanodomain inclusions observed in epoxy/BCP system using poly(styrene-*b*-butadiene-*b*-methacrylate) ABC terpolymer, depending on the BCP composition (Ritzenthaler et al. 2003)

Introduction of a fourth different block (ABCD) provides an extra level of complexity to the epoxy/BCP systems not even realized in epoxy/ABC terpolymer blends. Difficulty to control microphase separation of such complex systems may explain why there are only few works on epoxy/ABCD BCP blends. Rebizant et al. (2003) explored epoxy/BCP blends using PS-*b*-PB-PMMA-*b*-PGMA tetrablock copolymer. The authors succeeded to characterize raspberry-like morphologies bearing multi-domain microphase-separated structures.

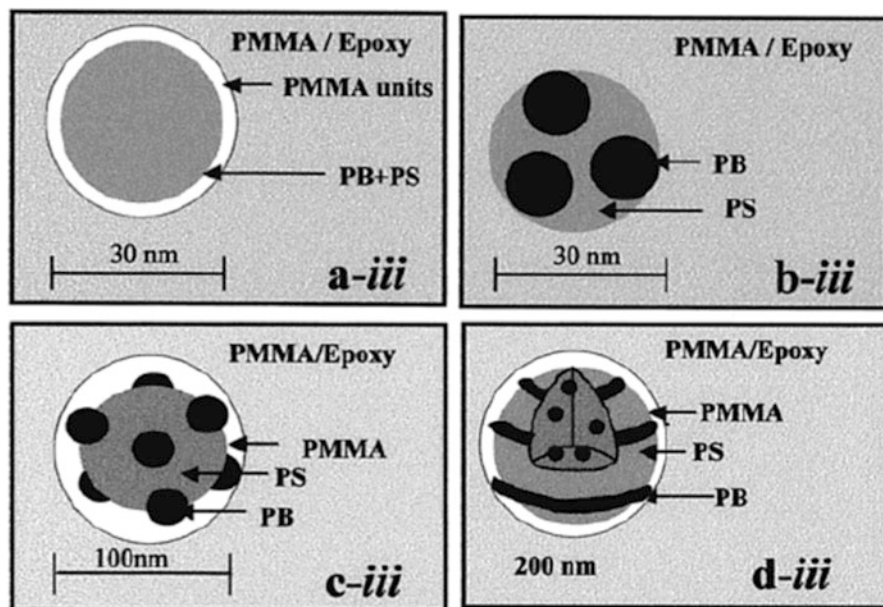


Fig. 14 Nanostructures obtained when ABC block copolymer (PS-*b*-PB-*b*-PMMA), where PMMA is the miscible block, in DGEBA/MCDEA system. (a) Spherical micelle, (b) sphere on sphere, and (c) core shell onion (Adapted with permission from Ritzenthaler et al. (2003). Copyright (2015). American Chemical Society)

Block Sequence

BCP architecture may influence the mechanism by which the BCP microphase separates within the epoxy system and, therefore, affect the final morphological pattern. For instance, Yu et al. (2012) investigated the morphological evolution of epoxy/BCP blends using PS-*b*-PCL (AB) diblock copolymer and PS-*b*-PCL-*b*-PS (ABA) triblock copolymer bearing identical block length. After systematic analysis by SAXS and AFM, the authors found that AB diblock copolymer formed spherical nanophases, whereas ABA triblock copolymer displayed vesicular nanodomains. Morphological differences were accounted to the different degrees of swelling of PCL blocks at the interfaces, as a consequence of changing the BCP architecture. PCL swelling with the epoxy precursors is associated with the PCL subchain conformation. In the AB configuration, PCL blocks displayed the conformation in which each PCL subchain is along the normal direction to the interface of PS nanodomains. In contrast, for the ABA architecture, PCL blocks adopted the loop-like conformation at the interface of PS microdomains, as depicted in Fig. 15. Therefore, the free-end PCL subchains in the AB diblock copolymer could accommodate epoxy precursors more than those for the ABA system, owing to the difference in the PCL subchain conformation. To meet this requirement of the interfacial curvature, AB block copolymer displayed sphere-like nanodomains while ABA block copolymer formed vesicular nanophases.

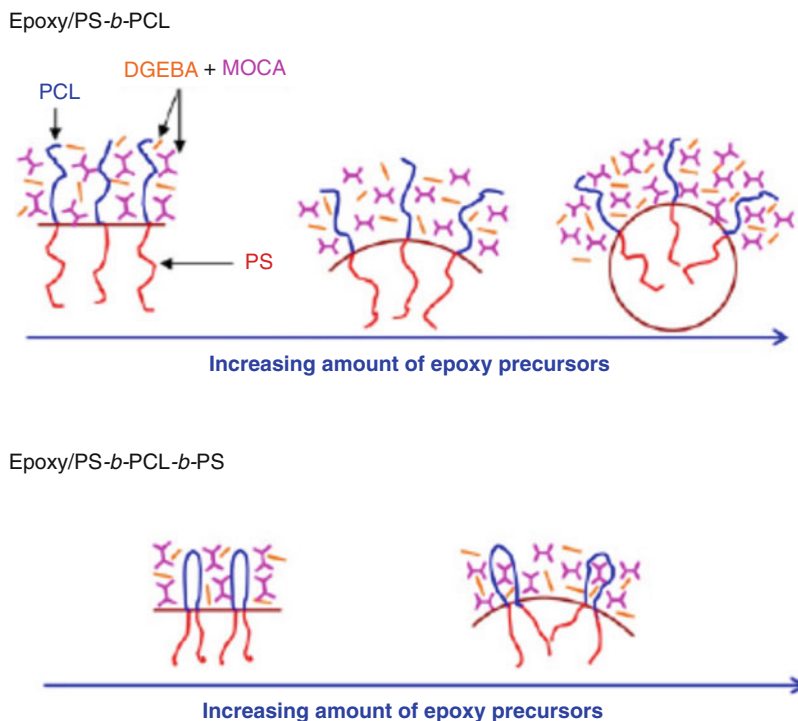


Fig. 15 Formation of nanophases in the thermosets containing PS-*b*-PCL diblock and/or PS-*b*-PCL-*b*-PS triblock copolymer in the process of curing reactions

Another interesting consequence of the block copolymer architecture is that described by Garate et al. for an epoxy/BCP blend using highly epoxidized SIS block copolymer (eSIS) (ABA architecture) (Garate et al. 2013). By following the morphological evolution of the system as the curing progressed, the authors observed that the initially spherical nanodomains became gradually distorted shifting to bigger and less organized nanostructures as a consequence of epoxidized poly(isoprene) (ePI) subchain local expulsion. Before curing, PS block self-assembled into spherical nanodomains, while ePI block remained swollen by the epoxy precursors. In this case, the configuration of ePI subchains was a combination of “loop-like” and “bridge-like” conformation due to the BCP composition (23 wt.%). In “bridge-like” conformation, ePI subchains are connecting two adjacent PS spherical nanodomains, as shown in Fig. 16 before curing. Under these conditions, “loop-like” ePI subchains were locally demixed to the surroundings of PS nanodomains, while “bridge-like” ePI subchains were not able to do so due to mobility restrictions imposed by PS blocks at each extreme. Therefore, “bridge-like” ePI subchains were partially demixed into the region between two interconnected PS nanodomains, as depicted in Fig. 16 after curing. These differences in local expulsion of ePI subchains with different configurations could explain the morphological shift from spherical to distorted sphere-like nanodomains in the systems investigated by Garate et al. (2013).

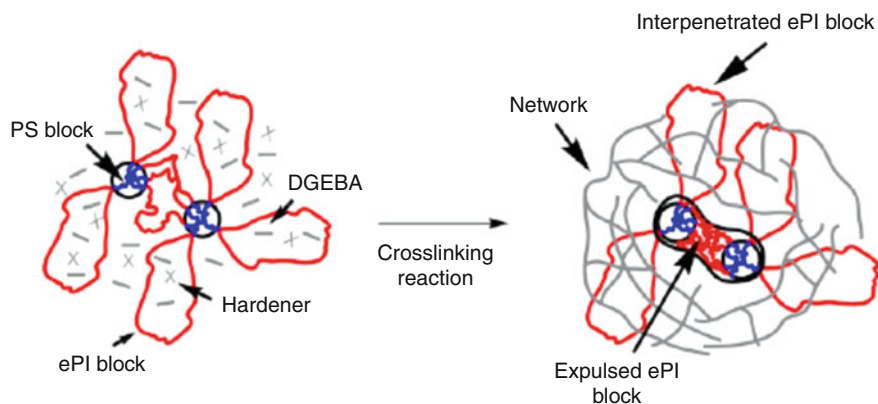


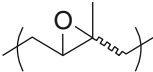
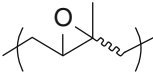
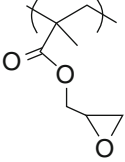
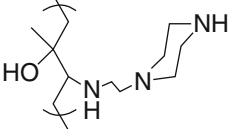
Fig. 16 Scheme of uncured (*left*) and cured (*right*) states for epoxy/eSIS85 blend

Influence of BCP Reactivity

Based on the nanostructuration mechanisms proposed by Grubbs et al. (2000), the reactivity of the BCP toward the epoxy precursors has great influence in the way the BCP microphase separates within the cross-linked matrix. The incorporation of any chemical group to the miscible block of the BCP capable of reacting with the thermosetting polymer during the curing cycle is a key parameter to control not only the morphology of the nanostructured nanocomposite, but also the interfacial adhesion between dispersed nanophases and the matrix. To obtain an optimum adhesion between the epoxy matrix and the block copolymer, Grubbs et al. and Dean et al. (Grubbs et al. 2000, 2001; Dean et al. 2003a, b) employed a different approach by incorporating functional groups into the block copolymer. The epoxy groups of glycidyl methacrylate in a poly(methyl acrylate-*stat*-glycidyl methacrylate-*block*-isoprene) block copolymer were able to react with the amine end groups of the hardener 4,4'-methylenedianiline (MDA), so that the block copolymer could cure within the epoxy network. In these works, glycidyl derivatives were considered as well as other oxiranes, since the reactivity of such units can enter in competition with the one of DGEBA. Of course that when incorporating reactive BCP, it is very important to adjust the stoichiometric balance between epoxy groups and $-NH$ groups of the hardener.

Following this idea, Rebizant et al. extended the possible functional spectrum by incorporating carboxylic reactive group after hydrolysis of *tert*-butyl methacrylate repeating units of a poly(styrene)-*b*-polybutadiene-*b*-poly[(methyl methacrylate)-*stat*-(*tert*-butyl methacrylate)] (Rebizant et al. 2004). This group was able to react with both epoxy and amine groups of the epoxy precursors. Rebizant et al. found that the formation of ether links by addition of $-COOH$ onto the oxirane ring is quick enough to prevent phase separation at the early stage of cure. The authors concluded that the formation of small amounts of graft in the early stage of the curing is sufficient to stabilize the interfaces and preserve the nanostructure until

Table 1 Reactive groups of block copolymers

Group	Reactive toward	Reaction conditions	References
	4,4'-methylenedianiline	55 °C for 48 h + 200 °C for 1 h	Grubbs et al. 2000
	1,3-bis(aminomethyl)benzene/1-(2-aminoethyl)piperazine (2:1 mol/mol)	80 °C for 3 h	Garate et al. 2013
	4,4'-methylenebis-(3-chloro 2,6-diethylaniline)	140 °C for 24 h + 165 °C for 2 h	Serrano et al. 2006
	4,4'-methylenedianiline	100 °C for 24 h + 210 °C for 1 h	Grubbs et al. 2000
	4,4'-diaminodiphenyl sulfone	135 °C for 5 h or 220 °C for 5 h	Rebizant et al. 2003
	4,4'-methylenedianiline	150 °C for 12 h + 180 °C for 2 h	Hameed et al. 2010
	4,4'-diaminodiphenyl sulfone	135 °C for 5 h	Rebizant et al. 2004
DGEBA	135 °C for 5 h		
	DGEBA	80 °C for 3 h	Garate et al. 2014

the gel point. More recently, Garate et al. arrived to a similar conclusion by blending an epoxy system with poly(styrene-*b*-epoxyisoprene-*b*-styrene) (eSIS) block copolymer bearing terminal amine groups (A-eSIS) (Garate et al. 2014). By this approach A-eSIS was more reactive toward the epoxy precursors compared to epoxidized SIS. By employing A-eSIS, sphere-like nanodomain morphology could be controlled, whereas eSIS displayed wormlike nanostructures by local expulsion of partially reactive ePI subchains.

These results demonstrate that the obtained nanostructure in an epoxy thermoset can be modulated by incorporating a BCP containing an epoxy-miscible block with enhanced reactivity toward the epoxy system (Table 1).

Influence of the Hardener

Selection of the hardener of an epoxy system is very important because it has great impact on the final properties of the cross-linked network. Epoxy systems are generally cured using difunctional nucleophilic molecules capable of reacting

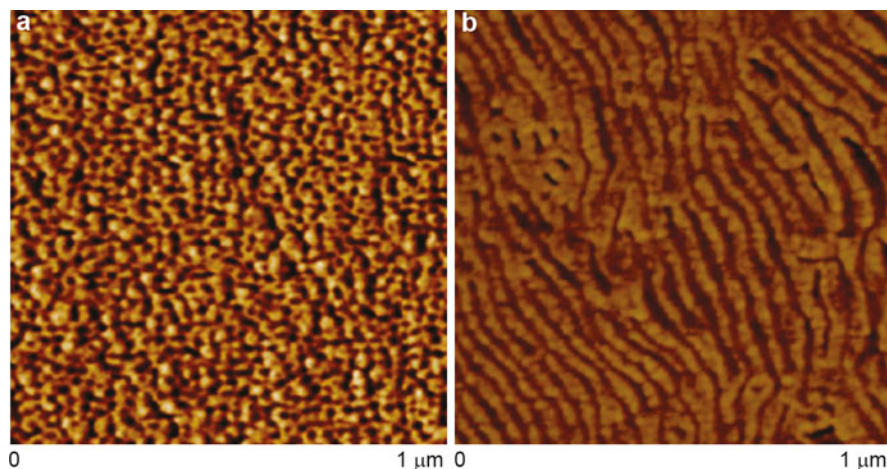


Fig. 17 AFM-phase contrast images of epoxy thermosets containing 30 wt.% of PEO-*b*-PCL-*b*-PS triblock copolymer with MOCA (a) and DDS (b) as hardener. Images correspond to $1 \mu\text{m} \times 1 \mu\text{m}$ area (Adapted with permission from Yu and Zheng (2011). Copyright (2011). American Chemical Society)

toward oxirane groups of the epoxy monomer (diamines, anhydrides, diphenols, among others). This section focuses on diamines, which are the most common hardeners employed for epoxy/BCP blends.

The nanostructures within epoxy/BCP blends can be modulated by the use of different hardener. In this regard, Yu et al. (Yu and Zheng 2011) investigated the impact of using 4,4'-methylenebis(2-chloroaniline) (MOCA) or 4,4'-diaminodiphenylsulfone as hardeners on the microphase separation behavior of epoxy/PEO-*b*-PS-*b*-PCL triblock copolymer blends. The authors found strong differences on the morphological pattern of the cured nanocomposites, as shown in Fig. 17. Thermosets cured with MOCA (Fig. 17a) presented a combination of spherical and wormlike PS microdomains, while for the samples cured with DDS (Fig. 17b), the thermosets displayed lamellar nanostructures.

In order to rationalize how the hardener influenced the final morphologies, the authors considered the following aspects: first, the impact of the selected hardener on the epoxy precursor solubility parameter. It is well known that the selection of the amine can increase the solubility of a BCP with the epoxy monomer (Fan et al. 2009) or, on the contrary, reduce the solubility of the BCP with the epoxy precursor (Garate et al. 2013), as for the case of amines with increased polarity. By means of SAXS the authors determined that epoxy/BCP blends in the uncured state were homogeneous when the hardener was 4,4'-methylene-bis-(2-chloroaniline). On the contrary, epoxy/BCP blends self-assembled into nanophases in the uncured state when the hardener was DDS. However, by heating the samples to the curing temperature, self-assembled structures disappeared due to UCST behavior of PS block in the mixture of epoxy precursors.

The second important aspect addressed by Yu et al. (Yu and Zheng 2011) is the ability of the cross-linked epoxy to establish intermolecular specific interactions with the miscible block of the BCP that stabilize the cross-linked network (i.e., hydrogen bonds). The authors stated that hydrogen bonds between carbonyl of PCL subchains and hydroxyl ether structural units of the epoxy network could be significantly suppressed by replacing MOCA for DDS due to the presence of considerable intramolecular hydrogen bonds between sulfonyl groups from DDS moieties and hydroxyl ether structural units of epoxy network. This stabilization difference would in turn give access to control whether PCL subchains remain in the wet-brush state or undergoes phase separation (dry brush) by PIMPS.

For the case of epoxy/BCP blends with reactive BCP, special consideration must be taken. In such systems, it is strongly recommended to perform separated analysis to determine the relative reactivity of BCP/hardener against epoxy monomer/hardener. To this end, depending on the nature of the amine (primary, secondary, aromatic, aliphatic), it is possible to tune the BCP/hardener reaction and therefore the phase separation behavior of the BCP within the epoxy matrix. For instance, George et al. (2014) investigated the system DGEBA-BCP blend using epoxidized poly(styrene-*b*-butadiene-*b*-styrene) eSBS block copolymer with an epoxidation degree of 47% and 4,4'-diaminodiphenylmethane (DDM) (*p*-substituted aniline) as hardener. Although epoxidized polybutadiene subchains contain secondary oxirane rings, the authors stated that no reaction occurred during curing between eSBS and DDM. On the contrary, Garate et al. (2013) employed a DGEBA/BCP blend using a highly epoxidized poly(styrene-*b*-isoprene-*b*-styrene) (eSIS85) block copolymer with an epoxidation degree of 85 wt.% cured with a more nucleophilic hardener than the *p*-substituted aniline used by George et al. (Kanzian et al. 2009). The hardener consisted of a mixture of 1,3-bis(aminomethyl)benzene (*m*-XDA) (primary diamine) and 1-(2-aminoethyl) piperazine (AEP) (primary-secondary-tertiary amine) (2:1 mol/mol). By means of fourier transform infrared spectroscopy (FT-IR) and differential scanning calorimetry (DSC) experiments, the authors found that the tertiary oxirane rings of epoxidized isoprene (ePI) units partially reacted with the hardener at the curing conditions, precluding a complete ePI subchain demixing process. Therefore, the nucleophilicity of the selected hardener is a very important aspect that has to be carefully considered to ascribe the correct microphase separation behavior of epoxy-reactive BCP blends.

Blending formulations to obtain nanostructured epoxy/BCP blends by the different microphase separation mechanisms detailed in this section is given in Table 2 (Fig. 18).

Influence of Curing Conditions

The possibility of trapping one of the evolving nanostructures generated during polymerization by control of the curing conditions can be of interest to modulate final properties of the material such as transparency and toughness, among others. The nanostructuration mechanism and the morphologies generated during polymerization of a specific blend may be strongly influenced by the presence of solvents or cosolvents and the selection of the curing temperature and the cure cycles.

Table 2 Epoxy/BCP blend formulation, microphase separation mechanism, cure cycle and morphology

Block copolymer	Epoxy system	Mechanism	Curing cycle	Morphology	BCP wt. %	References
No reactive, the miscible block is in bold						
PS- <i>b</i> -PMMA	DGEBA +MOCA	PIMPS	150 °C for 2 h + 180 °C for 2 h	S	10%	Fan and Zheng 2008
<i>star</i> -PS- <i>b</i> -PMMA	DGEBA +MOCA	PIMPS	150 °C for 2 h + 180 °C for 2 h	S+C	20%	Romeo et al. 2013
PEP- <i>b</i> -PEO	DGEBA +THPE	SA	200 °C for 2 h/60 °C for 40 min + 80 °C for 1 h + 120 °C for 2 h	L	40%	Fan and Zheng 2008
PEP- <i>b</i> -PEO	DER383, DER560 +PN	SA	200 °C for 2 h	S	5%	Liu et al. 2008; Thompson et al. 2009; Redline et al. 2014
			100 °C for 1 h + 125 °C for 1 h + 150 °C for 2 h	W	5%	Liu et al. 2010
PS- <i>b</i> -PEO	DGEBA +MOCA	PIMPS	150 °C for 2 h + 180 °C for 2 h	S+W	5%	Hermel-Davidock et al. 2007
PS- <i>b</i> -PEO	DGEBA +MDA	PIMPS	135 °C for 4 h	S	10%	Meng et al. 2006
<i>star</i> -PS- <i>b</i> -PCL	DGEBA +MOCA	PIMPS	150 °C for 2 h + 180 °C for 2 h	W	20%	Leonardi et al. 2015
				S	10%	Meng et al. 2008
PS- <i>b</i> -PCL	DGEBA +MOCA	PIMPS	150 °C for 2 h + 180 °C for 2 h	W	20–30%	
				L	40%	
PEO- <i>b</i> -PCL	DGEBA +MDA	SA	80 °C for 8 h + 150 °C for 2 h + 175 °C for 1 h	S	40%	He et al. 2014
PS- <i>b</i> -PB- <i>b</i> -PMMA	DGEBA +MCDEA	SA	135 °C for 24 h + 190 °C for 4 h	SS	50%	Ritzenthaler et al. 2002

(continued)

Table 2 (continued)

Block copolymer	Epoxy system	Mechanism	Curing cycle	Morphology	BCP wt. %	References
PS- <i>b</i> -PB- <i>b</i> -PMMA	DGEBA +MCDEA	SA	135 °C for 14 h (for 10% of BCP, for other BCB content 20, 24, or 185 h) + 190 °C for 4 h	S SS SS/CS	10% 15% ≥30%	Ritzenthaler et al. 2003
PEO- <i>b</i> -PCL- <i>b</i> -PS	DGEBA +MOCA	PIMPS	150 °C for 4 h + 180 °C for 2 h	S W	10% 30%	Yu and Zheng 2011
PEO- <i>b</i> -PCL- <i>b</i> -PS	DGEBA +DDS	PIMPS	150 °C for 4 h + 180 °C for 2 h	S L	20% ≥30%	Yu and Zheng 2011
PDMS- <i>b</i> -PCL- <i>b</i> -PS	DGEBA +MOCA	SA +PIMPS	150 °C for 2 h + 180 °C for 2 h	CS L	≤20% ≥30%	Fan et al. 2009
PCL- <i>b</i> -PEEES- <i>b</i> -PCL	DGEBA +MOCA	SA	150 °C for 3 h + 180 °C for 2 h	S W	10% ≥30%	Cong et al. 2014
PCL- <i>b</i> -PBS- <i>b</i> -PCL	DGEBA +MOCA	PIMPS	150 °C for 3 h + 180 °C for 2 h	S W	10% 40%	
PS- <i>b</i> -PCL- <i>b</i> -PBA	DGEBA +MOCA	PIMPS	150 °C for 4 h	S W	10–20% 30–40%	Fan et al. 2010
		PIMPS	150 °C for 4 h + 180 °C for 2 h	CS L	10–20% 30–40%	
PS- <i>b</i> -PB- <i>b</i> -P (MMA- <i>stat</i> -BMA)	DGEBA +MCDEA	SA	135 °C for 5 h	S	10%	Rebizant et al. 2004
PS- <i>b</i> -PB- <i>b</i> -P (MMA- <i>stat</i> -BMA)	DGEBA +DDS	SA	135 °C for 5 h	SS	30%	
PS- <i>b</i> -PB- <i>b</i> -P (MMA- <i>stat</i> -MAA)	DGEBA +DDS	SA	135 °C for 5 h	SS	30%	

Reactive, the reactive block is in bold								
PI-<i>b</i>-P4VP	DGEBA +MDA	PIMPS	100 °C for 20 h + 150 °C for 2 h + 175 °C for 1 h	S	5%			Guo et al. 2008
PS-<i>b</i>-ePB	DGEBA +MCDEA	SA +PIMPS	140 °C for 24 h + 165 °C for 2 h	V	10%			Ocando et al. 2009
				W	30%			
PS-<i>b</i>-ePB	DGEBA +MCDEA	PIMPS	140 °C for 24 h + 165 °C for 2 h	C	30%			Serrano et al. 2006
PB-<i>b</i>-ePI	BPA +MDA	SA +PIMPS	55 °C for 48 h + 200 °C for 1 h +	S	10–30%			Grubbs et al. 2000
				L	≥65%			
PI-<i>b</i>-P(MA-<i>co</i>-GMA)	BPA +MDA	PIMPS	100 °C for 24 h + 210 °C for 1 h	S	5%			
PS-<i>b</i>-PB-<i>b</i>-P(MMA-<i>stat</i>-MAA)	DGEBA +MCDEA	SA	135 °C for 5 h	S	10%			Rebizant et al. 2004
PS-<i>b</i>-PB-<i>b</i>-P(MMA-<i>stat</i>-MAA)	DGEBA +DDS	SA +PIMPS	135 °C for 5 h	S	30%			

S spherical, C cylinder, L lamellar, W wormlike, SS spheres on spheres, CS core shell, V vesicle

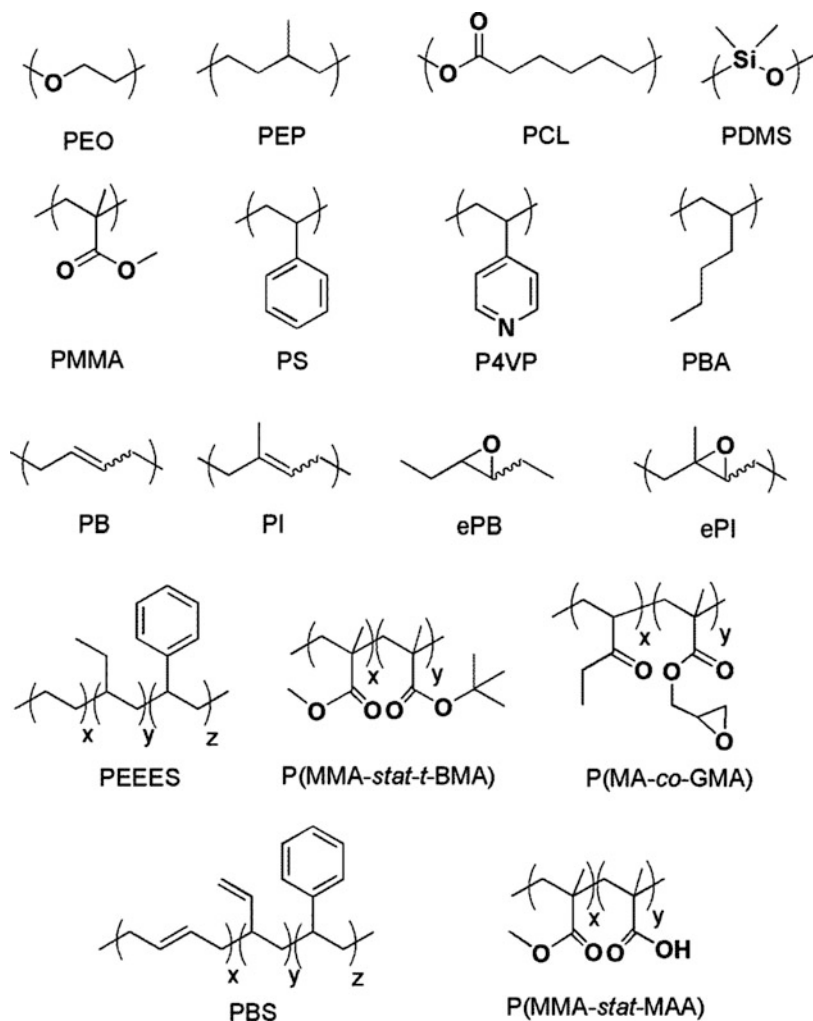


Fig. 18 Chemical structures of different blocks referred in Table 2

Solvents or Cosolvents

Epoxy/BCP blends can be prepared in bulk or as films depending on the application purpose. Protocols employed to obtain bulk or film samples generally require the use of a good solvent for the epoxy system and the BCP in order to attain a homogeneous mixture before curing. For bulk samples, it is essential to perform an intermediate of step solvent evaporation before curing (Serrano et al. 2006). Thus, volatile solvent are the preferred choice for this step. Of course that if the solvent is not adequately removed from the blend, the viscosity of the system could be low enough to allow an increase in the nanodomain coarsening rate. This may in turn alter the morphology dimensions and eventually could lead to macrophase

separation. A similar situation occurs for the case of coating applications (film samples). In this case solvents are generally needed to allow a good application of the material over the substrate. Once the material is applied, it is necessary to evaporate the solvent before curing for the same reasons explained for bulk samples (Dean et al. 2003a; Garate et al. 2011; Li et al. 2014).

Temperature

Curing temperature of course will affect the polymerization rate and the viscosity of the medium. On the one hand, increasing the polymerization rate may substantially reduce the available time for phase separation before reaching the gel point, and this can be beneficial for mechanisms initiated by SA, where it is desirable to preserve the original morphology. However, an increase in temperature also leads to a decrease in viscosity and therefore an increase in the coarsening rate of the self-assembled nanodomains.

The curing temperature will also determine whether a BCP undergoes SA or PIMPS mechanism. This is the case for those BCP bearing a block which displays UCST (i.e., polystyrene). If the selected curing temperature is below the UCST, SA mechanism may take place. On the contrary, if the curing temperature is above the UCST, the uncured state will be homogeneous, and the nanodomains will eventually be obtained by PIMPS mechanism.

Curing temperature selection is also critical for those epoxy/BCP blends where the BCP is reactive toward the epoxy precursor. For this case, it is very important to study which is the optimum reaction temperature for the epoxy precursors (i.e., DGEBA/hardener) and to compare this with the reaction between BCP and the epoxy precursor. Grubbs et al. (2000) studied the system poly(bisphenol A-*co*-epichlorohydrin)/4,4'-methylenedianiline modified by poly(1,2-butadiene)-*block*-poly(epoxy-1,4-isoprene-*ran*-1,4-isoprene) (BI87) BCP. By performing DSC experiments, the authors determined that the reaction exothermic peak between the epoxy monomer and MDA was between 131 °C and 145 °C, while the reaction exothermic peak between the BCP and MDA was 263–287 °C. Therefore, by setting the curing temperature at 55 °C for 48 h and 200 °C for 1 h, the authors concluded that the reaction of BCP with the hardener did not occur simultaneously with the cure of the epoxy precursors. In fact, during the first curing step, BCP/MDA reaction was practically neglected, and therefore it was suggested that the epoxidized block could undergo local expulsion followed by interfacial reaction during the second curing step. More recently, Garate et al. (2011) studied by DSC experiments the system DGEBA with a mixture of 1-(2-aminoethyl)piperazine and 1,3-bis(aminomethyl)benzene as the curing agent modified with eSIS85. The authors found that the exothermic peak for DGEBA/hardener was 80 °C, while for eSIS85/hardener was in the range of 65–105 °C. Therefore, they stated that even though the reactivity of the epoxy system is higher than that for the epoxidized block, at the curing temperature (80 °C) the BCP could react simultaneously with the epoxy precursors.

These examples evidence that the selection of the curing temperature for a given epoxy/BCP blend may have strong consequences on the nanostructuration mechanism and therefore on the morphological features displayed after curing.

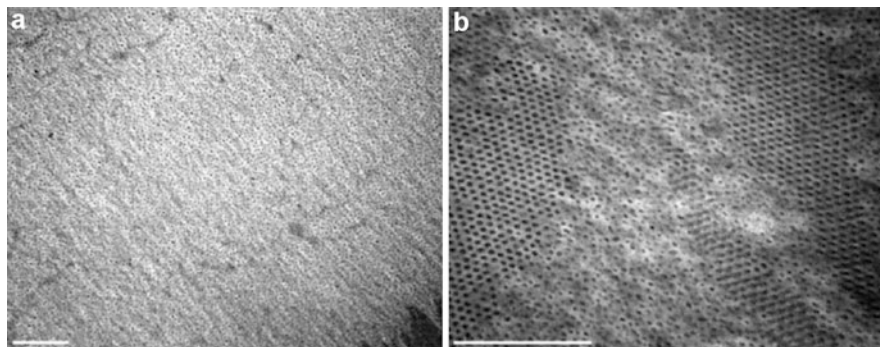


Fig. 19 TEM images of an epoxy/BCP blend reacted for 7 h at 135 °C and 4 h at 190 °C: (a) without the intermediate cooling to room temperature and (b) with intermediate cooling to room temperature. Scale bars = 1 μm (Reprinted with permission from Romeo et al. (2013). Copyright (2013). American Chemical Society)

Cure Cycle

The curing cycle can also be used to control the mechanism by which the BCP leads to the final morphology. In this regard, recent work by Romeo et al. (2013) pointed out the strong influence that the cure cycle may have on epoxy/BCP blends. The authors used an epoxy system formulated with DGEBA and 4,4'-methylenebis(2,6-diethylaniline) as the hardener modified with poly(styrene-*b*-methyl methacrylate). They employed two different curing cycles: (a) curing at 135 °C for 7 h followed by 190 °C for 4 h and (b) curing at 135 °C for 7 h followed by cooling to room temperature and 190 °C for 4 h. When the cure cycle was the condition *a*, a dispersion of spherical micelles and micellar chains were obtained (Fig. 19a). The introduction of a cooling step in the cure cycle (condition *b*) led to a dual-phase morphology consisting of microdomains of the hexagonal phase and regions exhibiting a dispersion of spherical micelles and micellar chains (Fig. 19b). The differences encountered were explained by the decrease of the miscibility of the PMMA block produced during the cooling step which produced partial phase separation of PMMA from the epoxy/amine network. Without the intermediate cooling step, the PMMA block remained interpenetrated within the cross-linked network and after the postcure was kinetically trapped in the final nanocomposite.

Impact of Morphology in the Epoxy/BCP Blend Properties

The obtained nanostructures in epoxy/amine matrix like sphere, cylindrical, worm-like micelle, and vesicle, among others, have an influence in the mechanical, thermal, and hydrophobic properties of the epoxy/BCP blends (Guo et al. 2002; Hameed et al. 2010; Cano et al. 2014; Zheng et al. 2014).

Mechanical Properties

One of the main interests of BCP to be used as epoxy modifiers relies in that they can improve fracture resistance of brittle epoxies even when they are added in relatively small amounts (<5 wt.%) (Dean et al. 2003a). Depending on to final morphology of the BCP in epoxy/amine matrix (vesicle, spherical micelles, or wormlike micelles), the improvement in the fracture resistance might be different. The fracture resistance, critical stress intensity factor (K_{Ic}), and the strain energy release rate have a strong dependence with the morphology of the BCP in the epoxy/amine matrix (Dean et al. 2003b; Cano et al. 2014).

Among the morphologies, vesicles are found to be more effective than spherical micelle to improve mechanical properties (Dean et al. 2001). Vesicles can be effective in toughening epoxy at relatively low loadings (2.5 wt.% block copolymer). Vesicles are closed, spherical objects consisting of a thin (ca. 10 nm) bilayer membrane that encases the epoxy resin. Given that the block copolymer forms only the shell and the volume of the vesicle phase consists of both the shell and the encapsulated epoxy, a small amount of block copolymer possess a large effective modifier volume fraction (Dean et al. 2003a).

In addition to vesicles and spherical micelles, block copolymers can also self-assemble into wormlike micelles according to the block copolymer architecture (Dean et al. 2003a). However, the improvement is bigger when wormlike micelle is employed (Dean et al. 2003b; Liu et al. 2010). Remarkably, addition of 5 wt.% block copolymer transforms the virtually useless fragile glassy material into a tough resistant plastic suitable for practical applications (Fig. 20). Wormlike micelles act as microcavities within the epoxy system, allowing more facile deformation of the matrix and therefore contributing to energy absorption. Additionally, it is possible to obtain a network of interconnected wormlike micelles which further enhances energy absorption in these materials (Wu et al. 2005).

The addition of BCP to an epoxy matrix produces generally a drop of Young's modulus while the fracture toughness increased. For similar BCP contents, vesicle morphology produces the largest decrease in Young's modulus which could be attributed to the large effective volume fraction of vesicles. A significant fraction of the cured epoxy resides inside the vesicle and does not fully contribute to the bulk Young's modulus of the blend (Thio et al. 2006).

Another important aspect to take into account is the nanoinclusion size developed during the BCP microphase separation. Small micelles neither induced plastic deformation nor contributed to surface roughness significantly whereas larger micelles acted as local defects resulting in early failure (Thio et al. 2009). There is an optimum inclusion length scale at which the toughening effect is maximized (Fig. 21), and this will depend on the particular system used (BCP, epoxy formulation, etc.).

Thermal Properties

Addition of BCP to the epoxy system may considerably alter the material glass transition temperature (T_g) value, and these changes depend on the BCP content

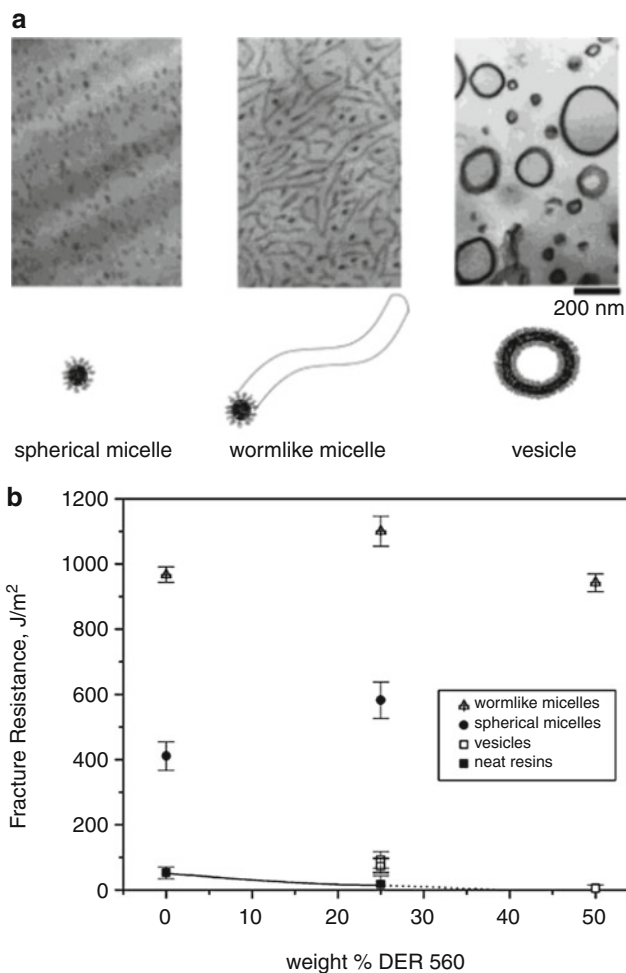


Fig. 20 (a) Different morphologies obtained for epoxy/amine network reinforced with PEO-PEP block copolymer, (b) fracture resistance of this mixtures containing 5 wt.% of block copolymer in diglycidyl ether of bisphenol A (DER383)/brominated diglycidyl ether of bisphenol A (DER560) epoxy system (Reprinted with permission from Dean et al. (2003b). Copyright (2003). American Chemical Society)

and the nanodomain morphology. For instance, by increasing BCP content, it is possible to shift the T_g to lower temperatures by means of the plasticization effect generated by nonreactive interpenetrated BCP subchains (Guo et al. 2002; Zhang et al. 2013; Cano et al. 2014). This effect seems to be more dependent on the BCP content than on the block ratio, as presented in Fig. 22 for epoxy/PEO-PPO-PEO blends with different EO contents and could be related with local decrease of epoxy cross-linking density as a consequence of the interpenetration of the miscible block.

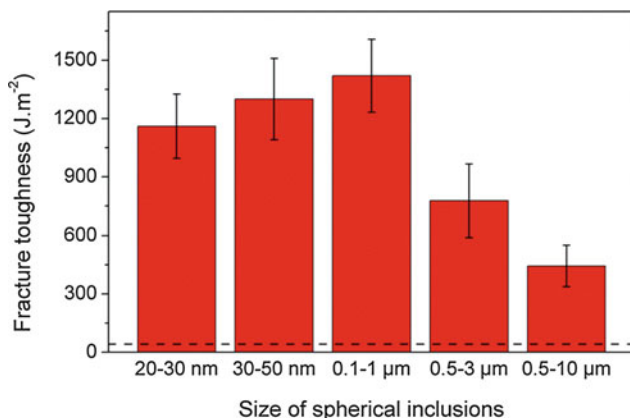


Fig. 21 Effect of the vesicle size morphology of poly(hexylene oxide-*b*-ethylene oxide) on the fracture toughness. The *dash line* corresponds to the epoxy system value

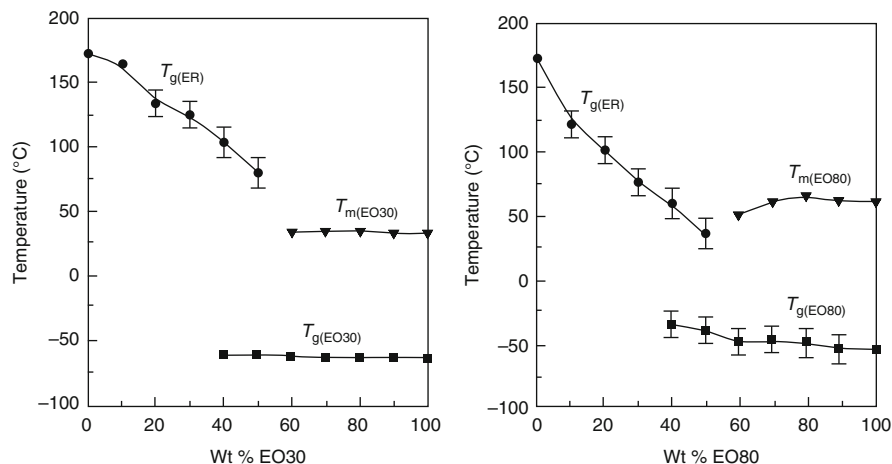
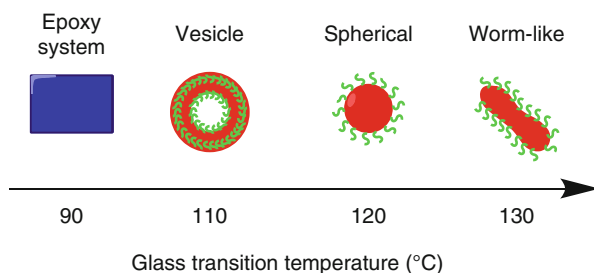


Fig. 22 T_g values for PEO-PPO-PEO blend epoxy resin ($T_{g(ER)}$) with different content of EO: 30 wt.% (*left*) and 80 wt.% (*right*). $T_m(EO)$ is the melting temperature, and $T_{g(EO)}$ is the T_g of the block copolymer, respectively (Reprinted with permission from Guo et al. (2002). Copyright (2002). American Chemical Society)

Other authors (Hameed et al. 2010; Garate et al. 2013) found that the incorporating reactive BCP to the epoxy system conducted to the opposite trend, shifting the T_g to higher values than that for the epoxy matrix. This effect occurs due to interpenetration and fixation of reactive BCP subchains. Once the BCP subchains are covalently linked to the epoxy matrix, demixing process is avoided, and therefore interpenetrated blocks can either fill matrix-free volume or increase the cross-linking density of the matrix. By doing so, the glass transition temperature is increased.

Fig. 23 Influence of the nanodomain morphology in the T_g of epoxy system for 5 wt.% of PBO-PEO modified epoxy



For the case of constant BCP content, the epoxy T_g value may have significant variations depending on the nanodomain morphology. Wu et al. (2005) observed that wormlike and spherical micelles conducted to a larger increment in T_g value than for the case of incorporating vesicles (Fig. 23). To rationalize this effect, it is important to consider that BCP addition perturbs the local concentration of epoxy precursors, because a little quantity of these components is solubilized inside the nanodomains. As long as the curing process occurs, the incorporated epoxy precursors are expelled from the swollen nanodomains to the epoxy-rich phase. This mass transport process depends on the interfacial area between the nanodomains and the continuous epoxy phase and therefore on the nature of the nanodomain morphology. This effect in combination with local expulsion of epoxy-miscible block at higher epoxy conversion is likely to alter the network topology and therefore constitute evident sources of variation in T_g , as pictured in Fig. 23.

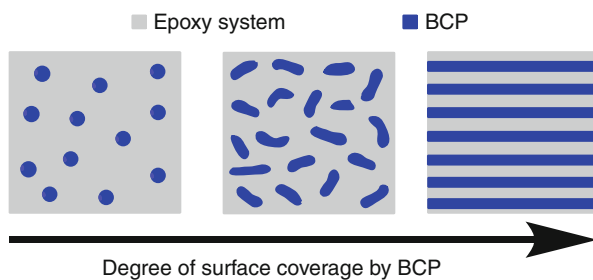
Surface Properties

Another important application of BCP as epoxy system modifier is the possibility of tuning material surface properties which is particularly relevant for coating applications. By properly selecting the BCP, the material surface property may be changed to more hydrophilic or hydrophobic for a specific application. This change in the epoxy system surface is gradual and increase with BCP content. The increment in BCP content produces two effects: (i) increment in epoxy covers area for the BCP and (ii) changes in the nanoinclusion morphology (Fig. 24).

The first effect determines the net change on hydrophobicity or hydrophilicity of epoxy system surface which depends of the block copolymer nature. For instance, the use of PDMS-PGMA (PDMS consists of a methacrylate siloxane hydrophobe) modifies the surface to more hydrophobic (Hameed et al. 2010). On the other hand, the use of PEO-PPO-PEO or PTFEMA-PCL-PTFEMA (PEO and PTFEMA have strong hydrophilic character) changes the surface to more hydrophilic (Cano et al. 2014; Zheng et al. 2014).

The second effect attains a nanoinclusion morphological shift from spheres to wormlike and from wormlike to lamellar structures, which in turn increases the BCP cover area exposed to the polymer/air interface.

Fig. 24 Epoxy system with different BCP contents



Conclusions

Different methods for generating nanostructured epoxy/BCP blends are discussed in this chapter. A general classification was proposed based on whether the solubility parameters of each block of the block copolymer are similar to those for epoxy precursors and therefore, on the basis of PIMPS mechanism, phase separation occurs during curing. On the other hand, if at least one block has a solubility parameter similar to those for the epoxy precursors but the other does not, microphase separation initiates before curing by self-assembly mechanism. Under the later condition, well-defined nanoinclusions are generated within the epoxy system, which are subsequently fixed by the growing epoxy network during curing. It was also discussed that by employing complex BCP other than simple symmetric diblock copolymers, the actual phase separation pathway may correspond to a combination of the previous mechanisms in a *tandem-like* way or simultaneously.

Both thermodynamics and kinetics of epoxy/BCP blends can be controlled by finely tuning epoxy formulation, BCP characteristics, and adequate curing conditions such as curing cycle and curing temperature, among others. These considerations must be carefully taken into account in order to gain control over the microphase separation mechanism and therefore over the nanodomain morphology displayed by the nanostructured system, as well as the final desired material properties.

References

- Amendt MA, Pitet LM, Moench S, Hillmyer MA (2012) Reactive triblock polymers from tandem ring-opening polymerization for nanostructured vinyl thermosets. *Polym Chem* 3:1827–1837
- Barton AFM (1990) Handbook of polymer-liquid interaction parameters and solubility parameters. CRC Press, Boca Raton
- Bates FS, Fredrickson GH (1999) Block copolymers-designer soft materials. *Phys Today* 52:32–38
- Bordes C, Fréville V, Ruffin E, Marote P, Gauvrit JY, Briançon S, Lantéri P (2010) Determination of poly(ϵ -caprolactone) solubility parameters: application to solvent substitution in a microencapsulation process. *Int J Pharm* 383:236–243

- Cano L, Builes DH, Tercjak A (2014) Morphological and mechanical study of nanostructured epoxy systems modified with amphiphilic poly(ethylene oxide-*b*-propylene oxide-*b*-ethylene oxide) triblock copolymer. *Polymer* 55:738–745
- Caseri W (2000) Nanocomposites of polymers and metals or semiconductors: historical background and optical properties. *Macromol Rapid Commun* 21:705–722
- Chen D, Pascault JP, Bertsch RJ, Drake RS, Siebert AR (1994) Synthesis, characterization, and properties of reactive liquid rubbers based on butadiene–acrylonitrile copolymers. *J Appl Polym Sci* 51:1959–1970
- Cong H, Li L, Zheng S (2014) Formation of nanostructures in thermosets containing block copolymers: from self-assembly to reaction-induced microphase separation mechanism. *Polymer* 55:1190–1201
- Dean JM, Lipic PM, Grubbs RB, Cook RF, Bates FS (2001) Micellar structure and mechanical properties of block copolymer-modified epoxies. *J Polym Sci Pol Chem* 39:2996–3010
- Dean JM, Grubbs RB, Saad W, Cook RF, Bates FS (2003a) Mechanical properties of block copolymer vesicle and micelle modified epoxies. *J Polym Sci Pol Chem* 41:2444–2456
- Dean JM, Verghese NE, Pham HQ, Bates FS (2003b) Nanostructure toughened epoxy resins. *Macromolecules* 36:9267–9270
- Declet-Perez C, Francis LF, Bates FS (2015) Deformation processes in block copolymer toughened epoxies. *Macromolecules* 48:3672–3684
- Esposito LH, Ramos JA, Mondragon I, Kortaberria G (2013) Nanostructured thermosetting systems modified with poly(isoprene-*b*-methyl methacrylate) diblock copolymer and polyisoprene-grafted carbon nanotubes. *J Appl Polym Sci* 129:1060–1067
- Esposito LH, Ramos JA, Kortaberria G (2014) Dispersion of carbon nanotubes in nanostructured epoxy systems for coating application. *Prog Org Coat* 77:1452–1458
- Fan W, Zheng S (2008) Reaction-induced microphase separation in thermosetting blends of epoxy resin with poly(methyl methacrylate)-*block*-polystyrene block copolymers: effect of topologies of block copolymers in morphological structures. *Polymer* 47:3157–3167
- Fan W, Wang L, Zheng S (2009) Nanostructures in thermosetting blends of epoxy resin with polydimethylsiloxane-*block*-poly(ϵ -caprolactone)-*block*-polystyrene ABC triblock copolymer. *Macromolecules* 42:327–336
- Fan W, Wang L, Zheng S (2010) Double reaction-induced microphase separation in epoxy resin containing polystyrene-*block*-poly(ϵ -caprolactone)-*block*-poly(*n*-butyl acrylate) ABC triblock copolymer. *Macromolecules* 43:10600–10611
- Garate H, Mondragon I, Goyanes S, D'Accorso N (2011) Controlled epoxidation of poly(styrene-*b*-isoprene-*b*-styrene) block copolymer for the development of nanostructured epoxy thermosets. *J Polym Sci Pol Chem* 49:4505–4515
- Garate H, Mondragon I, D'Accorso N, Goyanes S (2013) Exploring microphase separation behavior of epoxidized poly(styrene-*b*-isoprene-*b*-styrene) block copolymer inside thin epoxy coatings. *Macromolecules* 46:2182–2187
- Garate H, Goyanes S, D'Accorso N (2014) Controlling nanodomain morphology of epoxy thermosets modified with reactive amine-containing epoxidized poly(styrene-*b*-isoprene-*b*-styrene) block copolymer. *Macromolecules* 47:7416–7423
- George SM, Puglia D, Kenny JM, Parameswaranpillai J, Thomas S (2014) Reaction-Induced phase separation and thermomechanical properties in epoxidized styrene-*block*-butadiene-*block*-styrene triblock copolymer modified epoxy/DDM system. *Ind Eng Chem Res* 53:6941–6950
- Grubbs RB, Dean JM, Broz ME, Bates FS (2000) Reactive block copolymers for modification of thermosetting epoxy. *Macromolecules* 33:9522–9534
- Grubbs RB, Dean JM, Bates FS (2001) Methacrylic block copolymers through metal-mediated living free radical polymerization for modification of thermosetting epoxy. *Macromolecules* 34:8593–8595
- Guo Q, Thomann R, Gronski W (2002) Phase behavior, crystallization, and hierarchical nanostructures in self-organized thermoset blends of epoxy resin and amphiphilic poly

- (ethylene oxide)-*block*-poly(propylene oxide)-*block*-poly(ethylene oxide) triblock copolymers. *Macromolecules* 35:3133–3144
- Guo Q, Liu J, Chen L, Wang K (2008) Nanostructures and nanoporosity in thermoset epoxy blends with an amphiphilic polyisoprene-*block*-poly(4-vinyl pyridine) reactive diblock copolymer. *Polymer* 49:1737–1742
- Hameed N, Guo Q, Xu Z, Hanley TL, Mai Y-W (2010) Reactive block copolymer modified thermosets: highly ordered nanostructures and improved properties. *Soft Matter* 6:6119–6129
- He X, Liu Y, Zhang R, Wu Q, Chen T, Sun P, Wang X, Xue G (2014) Unique interphase and cross-linked network controlled by different miscible blocks in nanostructured epoxy/block copolymer blends characterized by solid-state NMR. *J Phys Chem C* 118:13285–13299
- Hedrick JL, Miller RD, Hawker CJ, Carter KR, Volksen W, Yoon DY, Trollsås M (1998) Templating nanoporosity in thin-film dielectric insulators. *Adv Mater* 10:1049–1053
- Hermel-Davidock TJ, Tang HS, Murray DJ, Hahn S (2007) Control of the block copolymer morphology in templated epoxy thermosets. *J Polym Sci Pol Phys* 45:3338–3348
- Hillmyer MA, Lipic PM, Hajduk DA, Almdal K, Bates FS (1997) Self-assembly and polymerization of epoxy resin-amphiphilic block copolymer nanocomposites. *J Am Chem Soc* 119:2749–2750
- Hu D, Zheng S (2009) Reaction-induced microphase separation in epoxy resin containing polystyrene-*block*-poly(ethylene oxide) alternating multiblock copolymer. *Eur Polym J* 45:3326–3338
- Kanzian T, Nigst TA, Maier A, Pichl S, Mayr H (2009) Nucleophilic reactivities of primary and secondary amines in acetonitrile. *Eur J Org Chem* 2009:6379–6385
- Karger-Kocsis J, Frölich J, Gryshchuk O, Kautz H, Frey H, Mülhaupt R (2004) Synthesis of reactive hyperbranched and star-like polyethers and their use for toughening of vinylurethane hybrid resins. *Polymer* 45:1185–1195
- Leonardi AB, Zucchi IA, Williams RJJ (2015) Generation of large and locally aligned wormlike micelles in block copolymer/epoxy blends. *Eur Polym J* 65:202–208
- Li T, Heinzer MJ, Redline EM, Zuo F, Bates FS, Francis LF (2014) Microstructure and performance of block copolymer modified epoxy coatings. *Prog Org Coat* 77:1145–1154
- Lipic PM, Bates FS, Hillmyer MA (1998) Nanostructured thermosets from self-assembled amphiphilic block copolymer/epoxy resin mixtures. *J Am Chem Soc* 120:8963–8970
- Liu J, Sue HJ, Thompson ZJ, Bates FS, Dettloff M, Jacob G, Verghese N, Pham H (2008) Nanocavitation in self-assembled amphiphilic block copolymer-modified epoxy. *Macromolecules* 41:7616–7624
- Liu J, Thompson ZJ, Sue H-J, Bates FS, Hillmyer MA, Dettloff M, Jacob G, Verghese N, Pham H (2010) Toughening of epoxies with block copolymer micelles of wormlike morphology. *Macromolecules* 43:7238–7243
- Mai Y, Eisenberg A (2012) Self-assembly of block copolymers. *Chem Soc Rev* 41:5969–5985
- Maiez-Tribut S, Pascault JP, Soule ER, Borrajo J, Williams RJJ (2007) Nanostructured epoxies based on the self-assembly of block copolymers: a new miscible block that can be tailored to different epoxy formulations. *Macromolecules* 40:1268–1273
- Matsen MW, Bates FS (1996) Unifying weak-and strong-segregation block copolymer theories. *Macromolecules* 29:1092–1098
- Meng F, Zheng S, Li H, Liang Q, Liu T (2006) Formation of ordered nanostructures in epoxy thermosets: a mechanism of reaction-induced microphase separation. *Macromolecules* 39:5072–5080
- Meng F, Xu Z, Zheng S (2008) Microphase separation in thermosetting blends of epoxy resin and poly(ϵ -caprolactone)-*block*-polystyrene block copolymers. *Macromolecules* 41:1411–1420
- Mijovic J, Shen M, Wing Sy J, Mondragon I (2000) Dynamics and morphology in nanostructured thermoset network/block copolymer blends during network formation. *Macromolecules* 33:5235–5244
- Mikos AG, Peppas NA (1988) Flory interaction parameter χ for hydrophilic copolymers with water. *Biomaterials* 9:419–423

- Ng SC, Chee KK (1997) Solubility parameters of copolymers as determined by turbidimetry. *Eur Polym J* 33:749–752
- O'Driscoll S, Demirel G, Farrell RA, Fitzgerald TG, O'Mahony C, Holmes JD, Morris MA (2011) The morphology and structure of PS-*b*-P4VP block copolymer films by solvent annealing: effect of the solvent parameter. *Polym Adv Technol* 22:915–923
- Ocando C, Tercjak A, Martín MD, Ramos JA, Campo M, Mondragon I (2009) Morphology development in thermosetting mixtures through the variation on chemical functionalization degree of poly(styrene-*b*-butadiene) diblock copolymer modifiers. *Thermomech Prop Macromol* 42:6215–6224
- Rebizant V, Abetz V, Tournilhac F, Court F, Leibler L (2003) Reactive tetrablock copolymers containing glycidyl methacrylate. Synthesis and morphology control in epoxy-amine networks. *Macromolecules* 36:9889–9896
- Rebizant V, Venet A-S, Tournilhac F, Girard-Reydet E, Navarro C, Pascault J-P, Leibler L (2004) Chemistry and mechanical properties of epoxy-based thermosets reinforced by reactive and nonreactive SBMX block copolymers. *Macromolecules* 37:8017–8027
- Redline EM, Declat-Perez C, Bates FS, Francis LF (2014) Effect of block copolymer concentration and core composition on toughening epoxies. *Polymer* 55:4172–4181
- Ritzenthaler S, Court F, David L, Girard-Reydet E, Leibler L, Pascault JP (2002) ABC triblock copolymers/epoxy-diamine blends. 1. Keys to achieve nanostructured thermosets. *Macromolecules* 35:6245–6254
- Ritzenthaler S, Court F, David L, Girard-Reydet E, Leibler L, Pascault JP (2003) ABC triblock copolymers/epoxy-diamine blends. 2. Parameters controlling the morphologies and properties. *Macromolecules* 36:118–126
- Romeo H, Zucchi I, Rico M, Hoppe CE, Williams RJJ (2013) From spherical micelles to hexagonally packed cylinders: the cure cycle determines nanostructures generated in block copolymer/epoxy blends. *Macromolecules* 46:4854–4861
- Serrano E, Larrañaga M, Remiro PM, Mondragon I, Carrasco PM, Pomposo JA, Mecerreyes D (2004) Synthesis and characterization of epoxidized styrene-butadiene block copolymers as templates for nanostructured thermosets. *Macromol Chem Phys* 205:987–996
- Serrano E, Tercjak A, Kortaberria G, Pomposo JA, Mecerreyes D, Zafeiropoulos NE, Stamm M, Mondragon I (2006) Nanostructured thermosetting systems by modification with epoxidized styrene-butadiene star block copolymers. Effect of epoxidation degree. *Macromolecules* 39:2254–2261
- Serrano E, Tercjak A, Ocando C, Larrañaga M, Parellada MD, Corona-Galván S, Mecerreyes D, Zafeiropoulos NE, Stamm M, Mondragon I (2007) Curing behavior and final properties of nanostructured thermosetting systems modified with epoxidized styrene-butadiene linear diblock copolymers. *Macromol Chem Phys* 208:2281–2292
- Thio YS, Wu J, Bates FS (2006) Epoxy toughening using low molecular weight poly (hexylene oxide)-poly (ethylene oxide) diblock copolymers. *Macromolecules* 39:7187–7189
- Thio YS, Wu J, Bates FS (2009) The role of inclusion size in toughening of epoxy resins by spherical micelles. *J Polym Sci Pol Chem* 47:1125–1129
- Thompson ZJ, Hillmyer MA, Liu J, Sue H-J, Dettloff M, Bates FS (2009) Block copolymer toughened epoxy: role of cross-link density. *Macromolecules* 42:2333–2335
- Van Krevelen DW (1990) *Properties of polymers*, 3rd edn. Elsevier, Amsterdam
- Verchère D, Sautereau H, Pascault JP, Moschiar SM, Riccardi CC, Williams RJJ (1989) *Polymer* 30:107–115
- Williams RJJ, Rozenberg BA, Pascault J-P (1997) Reaction-induced phase separation in modified thermosetting polymers. In: Abe A, Albertsson AC, Coates GW, Genzer J, Kobayashi S, Lee K-S, Leibler L, Long TE, Möller M, Okay O, Percec V, Tang BZ, Terentjev EM, Vicent MJ, Voit B, Wiesner U, Zhang X (eds) *Advances in polymer science*. Springer, Berlin, pp 95–156
- Wu J, Thio YS, Bates FS (2005) Structure and properties of PBO–PEO diblock copolymer modified epoxy. *J Polym Sci Pol Chem* 43:1950–1965

- Xu Z, Zheng S (2007) Morphology and thermomechanical properties of nanostructured thermosetting blends of epoxy resin and poly(ϵ -caprolactone)-*block* polydimethylsiloxane-*block*-poly(ϵ -caprolactone) triblock copolymer. *Polymer* 48:6134–6144
- Yu R, Zheng S (2011) Morphological transition from spherical to lamellar nanophases in epoxy thermosets containing poly(ethylene oxide)-*block*-poly(ϵ -caprolactone)-*block*-polystyrene triblock copolymer by hardeners. *Macromolecules* 44:8546–8557
- Yu R, Zheng S, Li X, Wang J (2012) Reaction-induced microphase separation in epoxy thermosets containing block copolymers composed of polystyrene and poly(ϵ -caprolactone): influence of copolymer architectures on formation of nanophases. *Macromolecules* 45:9155–9168
- Yu Y, Dubois P, Teyssié P, Jérôme R (1997) Difunctional initiator based on 1,3-diisopropenylbenzene.6. Synthesis of methyl methacrylate – butadiene – methyl methacrylate triblock copolymers. *Macromolecules* 30:4254–4261
- Zhang C, Li L, Zheng S (2013) Formation and confined crystallization of polyethylene nanophases in epoxy thermosets. *Macromolecules* 46:2740–2753
- Zheng Y, Xue Q, Zhu L, Xin Z, Sheng Y, Ren W (2014) Copolymer architecture effects on the morphology and surface performance of epoxy thermosets containing fluorinated block copolymers. *J Polym Sci Pol Phys* 52:1037–1045
- Zhu B, Katsoulis DE, Keryk JR, McGarry FJ (2004) Toughening of polysilsesquioxane network by simultaneous incorporation of short and long PDMS chain segments. *Macromolecules* 37:1455–1462